



HAL
open science

**Merging experimental design and structural
identification around the concept of modified
Constitutive Relation Error in low-frequency dynamics
for enhanced structural monitoring**

Matthieu Diaz, Pierre-Étienne Charbonnel, Ludovic Chamoin

► **To cite this version:**

Matthieu Diaz, Pierre-Étienne Charbonnel, Ludovic Chamoin. Merging experimental design and structural identification around the concept of modified Constitutive Relation Error in low-frequency dynamics for enhanced structural monitoring. *Mechanical Systems and Signal Processing*, 2023, 197, pp.110371. 10.1016/j.ymssp.2023.110371 . hal-03878634v2

HAL Id: hal-03878634

<https://hal.science/hal-03878634v2>

Submitted on 18 Apr 2023

HAL is a multi-disciplinary open access archive for the deposit and dissemination of scientific research documents, whether they are published or not. The documents may come from teaching and research institutions in France or abroad, or from public or private research centers.

L'archive ouverte pluridisciplinaire **HAL**, est destinée au dépôt et à la diffusion de documents scientifiques de niveau recherche, publiés ou non, émanant des établissements d'enseignement et de recherche français ou étrangers, des laboratoires publics ou privés.

Merging experimental design and structural identification around the concept of modified Constitutive Relation Error in low-frequency dynamics for enhanced structural monitoring

M. Diaz^{a,*}, P.-É. Charbonnel^b, L. Chamoin^{a,c}

5 ^aUniversité Paris-Saclay, CentraleSupélec, ENS Paris-Saclay, LMPS - Laboratoire de Mécanique Paris-Saclay, 91190, Gif-sur-Yvette, France

^bDES-Service d'Études Mécaniques et Thermiques (SEMT), CEA, Université Paris-Saclay, 91191 Gif-sur-Yvette, France

^cIUF, Institut Universitaire de France

10 Abstract

This paper presents a novel Optimal Sensor Placement (OSP) strategy that is dedicated to model updating problems based on the modified Constitutive Relation Error (mCRE) functional in low-frequency dynamics. The mCRE is a credible alternative to model updating functionals that stands out by searching structural parameters alongside mechanical fields as the best trade-off between all available information from measured data, without any further *a priori* assumption. Considering damage detection problems, due to possible discrepancies in terms of parameters sensitivity with respect to mCRE, sensor locations provided by standard OSP algorithms may be irrelevant. The proposed approach uses the concept of Information Entropy by formulating a modified Fisher information matrix, in which the sensitivity of the mCRE mechanical fields with respect to the updated parameters is involved. The approach is legitimated by the strong connection between mCRE and Bayesian inference. A proof-of-concept involving an earthquake engineering inspired academic case study, where accelerometers are positioned on a two-story frame structure subjected to random ground motion, permits to illustrate the soundness and efficiency of the proposed methodology compared to other classical OSP techniques. The influence of critical mCRE parameters is shown, as well as the benefits of taking multiple scenarios into account so as to get an OSP that is relevant for a wider range of possible damage occurrences.

Keywords: Optimal Sensor Placement, Modified Constitutive Relation Error, Structural Health Monitoring, Damage Detection, Earthquake Engineering.

*Corresponding author

Email address: matthieu.diaz@ens-paris-saclay.fr (M. Diaz)

List of abbreviations

SHM	Structural Health Monitoring
OSP	Optimal Sensor Placement
pdf	Probability Density Function
FIM	Fisher Information Matrix
FSSP	Fast Sequential Sensor Placement
BSSP	Backward Sequential Sensor Placement
mCRE	modified Constitutive Relation Error
CRE	Constitutive Relation Error

1. Introduction

15 Structural Health Monitoring (SHM) aims to improve the diagnosis of structures in operational conditions in order to prevent potential structural failures. If the monitoring operation was traditionally performed visually by human inspectors, the automated techniques that have been developed in the last four decades, which directly exploit data acquired by a set of sensors, make it possible to assist and reinforce the visual inspection carried out on structures in order to
20 permit a safe decision-making process. SHM has been particularly studied in the context of localizing, quantifying, and tracking structural damage from ambient dynamic datasets. Throughout the last decades, a broad panel of damage detection methods has been proposed [1–4] - only to cite a few of them. These techniques all have in common the aim of updating numerical models, whether they are directly built from measurements (*black-box modeling*) or derived after an
25 in-depth physical description of the involved phenomena (*white-box modeling*). These latter are then post-processed to extract valuable information regarding the current mechanical state of the sensed specimen, for instance, stiffness loss or modal feature changes [5, 6].

When performing model updating from (possibly spatially sparse) datasets, several difficulties have been identified [7–9]:

- 30 (i) Model bias due to the fact that the chosen class of structural models does not contain the actual behavior of the structure;
- (ii) Measurement noise in the dynamic test data that implies the addition of *a priori* information for regularization purposes;
- (iii) Incomplete observability of the structure due to the limited budget and technologies of
35 available sensing devices, leading to local and incomplete datasets;
- (iv) Incomplete number of contributing modes due to limited bandwidth in the input and dynamic response.

As difficulties (i) and (iv) are already addressed throughout the model updating framework considered in this contribution, we will mainly focus on the difficulty (iii) as one shall imagine
40 how inappropriate experimental designs can lead to inaccurate identification results.

The will to exploit at best the information provided by a few amount of sensors lead to the development of optimal sensor placement (OSP) techniques. Indeed, the quality of damage diagnosis from structural vibrations critically depends on the sensor layout, in particular considering large structures under unknown or random excitation that cannot be fully instrumented
45 in practice. As part of the experimental design, OSP is a challenging problem: as sensors are not properly positioned yet, the performance of OSP algorithms is thus conditioned by the (assumed good) predictive behavior of the involved numerical models that allow to generate simulated data. The question of sensor placement is not new [10, 11] and has been massively studied in the last three decades for SHM applications [12–15] with the introduction of a wide
50 variety of OSP criteria and optimization algorithms.

In SHM and structural dynamics applications, OSP problems were initially raised for modal identification purposes [16], as it has been historically well-known that damage occurrence was strongly related to eigenfrequencies loss and mode shapes change [17]. Considering parameter estimation of structures subjected to earthquake loading conditions, the mathematical expression of the OSP problem [18–20] introduced the Fisher Information Matrix (FIM) from the Cramér-Rao bound theorem. The FIM is a relevant mathematical entity on which the sensor selection process can rely: it measures the amount of information carried by a given sensor configuration (since it is strongly related to the sensitivity of model predictions with respect to the updated parameters). OSP algorithms then differ in the criterion/measure derived from the FIM. The most common approaches are either based on its trace (A-optimality) [16, 20–22], its condition number (E-optimality) [23], or its determinant (D-optimality) [19, 24].

Contrary to the previous OSP techniques that are based on modal features, the Bayesian framework proposed by Beck and Katafygiotis [25, 26] has been used to get OSP for structural identification by Papadimitriou [27] using the concept of information entropy. It benefits from the Bayesian statistical framework as it properly handles measurement uncertainties as well as model errors. A significant mathematical result relates asymptotically (*i.e.* for a large amount of data) the information entropy to the determinant of the FIM [28].

From these pioneering works, the research in OSP in the last decade has mostly been focused on optimization algorithms, as optimal sensor placement is a challenging problem from the computational viewpoint which resorts to combinatorial optimization. Efficient algorithms (that may provide sub-optimal results) are often used. They can be distinguished into two families. On the one hand, metaheuristic algorithms such as genetic algorithms are most suitable for solving discrete optimization problems and providing near-optimal solutions to global optimization problems [24, 27]. Among many contributions, let us mention [29, 30] that use genetic algorithms to optimally position sensors for damage detection. Of course, other metaheuristic techniques can be used for sensor placement such as neural networks [31, 32], topology optimization-inspired algorithms [33, 34], simulated annealing [31, 35] or mixed variable programming [36]. A comprehensive review of these techniques is given in [15]. On the other hand, sequential sensor placement techniques, whether they are forward (FSSP) or backward (BSSP), do only provide suboptimal sensor configurations. However, they are much less computationally demanding compared to genetic algorithms. In practice, sensors location are determined iteratively by placing/removing one sensor at a time. Although the effective independence method [19] lies on a BSSP strategy, FSSP and BSSP have strongly been popularized with information entropy [28, 37, 38]. It has been shown that FSSP and BSSP provide a good approximation (yet suboptimal) of the OSP on many test cases with less computational effort than genetic algorithms.

The ambition of this work is to enlarge the wide spectrum of OSP techniques with a novel strategy that is dedicated to the use of the modified Constitutive Relation Error functional (mCRE) for finite element model updating. Indeed, if the mCRE has been shown to be a relevant alternative to standard deterministic and stochastic model updating techniques [39, 40], no proper strategy devoted to mCRE-based model updating has been proposed in the literature.

Briefly, the mCRE is an alternative technique to solve inverse problems that are classically addressed using either Bayesian approaches (for which a comprehensive review is available in [5]) or deterministic methods [7, 41]. In these latter approaches, the need for regularization techniques is mandatory to circumvent the ill-posedness of the problem [8]. The regularization includes some user’s *a priori* expertise of paramount importance as it conditions the obtained solution and the convergence of the optimization algorithms [42, 43]. Although easy to implement, these techniques may lack of robustness as the identification result is strongly relying on (i) the choice of the *a priori* information that regularizes the inverse problem in Tikhonov’s sense, and (ii) the calibration of the relative weights of the different terms contributing to the

cost function [44]. An alternative then consists in using the concept of modified Constitutive Relation Error (mCRE) whose physics-based construction avoids the need for user-dependent knowledge [45–47]. This is the main driver behind its selection as a reference method for model updating in this paper.

105 Initially proposed for model updating in dynamics by Ladevèze and co-workers [48, 49], the mCRE functional is defined as a quadratic data-to-model distance enriched with a term based on the concept of Constitutive Relation Error (CRE) [50]. This CRE term is built from the reliability of information concept, and therefore carries a strong mechanical content. In particular, it allows to avoid the direct use of regularization terms based on some *a priori* expert-
110 user knowledge. Compared to standard deterministic and stochastic functionals, the mCRE is known for having enhanced convexity properties [51] and high-robustness to measurement noise [47, 52]. Besides, the elementary contributions of the model error term can be easily computed and exploited to focus updating actions where needed [53]. This can be computationally helpful and regularizing (in Tikhonov’s sense) when the sensitivity of the mCRE with respect to updated
115 parameters is heterogeneous. The relevance and robustness of the mCRE for model updating have been emphasized in many applications. Among other works, let us mention local defect detection [46, 54, 55], full-field material identification from dense measurements [56, 57], and model updating from low signal-to-noise ratio random measurements in dynamics [47]. As one can explicitly establish a link between mCRE, deterministic and stochastic functionals, it is
120 also worth mentioning the comparative study between mCRE, Tikhonov-based, and Bayesian damage detection using optical fiber strain measurements performed in [39]. Another comparison was performed from full-field measurements obtained by digital image correlation in which the benefits of using mCRE compared to Bhattacharyya distance were observed [40].

If the modeling error distribution over the structure can be advantageously used to position
125 sensors in areas that are in need for correcting actions, such an approach remains empirical and lacks of mathematical foundations to be properly generalized. The main contribution of this work consists in the development of a novel sensor placement strategy that integrates the mCRE within the information theory, which is legitimated by the mathematical relationship between mCRE and Bayesian model updating when dealing with Gaussian random variables.
130 A modified FIM is formulated and its determinant is maximized to position sensors optimally for enhanced mCRE-based monitoring in low-frequency dynamics. A proof-of-concept showing the relevance of this new mCRE-based OSP strategy is proposed on a 3D academic example, in which accelerometers are optimally positionned on a two-story frame structure. This case study allowed to compare the new mCRE-based OSP approach with other classical techniques:
135 the relevance of OSPs is assessed in terms of identification accuracy using measurements from different scenarios and relative uncertainties quantified with confidence intervals [53]. The effect of the confidence into measurements coefficient is particularly considered as the calibration of the latter is crucial within the mCRE framework [47], and physically-meaningful observations are made when analyzing its impact on OSP results. The case of multiple damage scenarios is
140 also considered, showing that the additional computational burden carried by such an approach yet enables obtaining more relevant OSP leading to better model updating, even when the parameters to identify are subjected to significant evolutions during experiments.

The remainder of this paper is organized as follows: Section 2 presents an overview of
145 OSP techniques dealing with the concept of FIM, with particular emphasis on the information entropy concept. Section 3 recalls the basics of the mCRE for finite element model updating in dynamics. Section 4 presents the novel sensor placement approach starting from the mCRE seen from a Bayesian viewpoint. Section 5 presents the proof-of-concept showing the relevance of the proposed OSP method. Conclusions and prospects are finally drawn in Section 6, suggesting a future use of this novel OSP technique for a model updating framework unified around the
150 concept of mCRE.

2. Optimal sensor placement techniques for SHM at a glance

In this section, the most common and popular sensor placement techniques are briefly presented. Although OSP problems were originally raised for modal identification purposes, the tools that are invested are (for the largest part) all related to the information theory, which will be presented in the following. For the sake of conciseness and clarity, only the material essential to the forthcoming developments is detailed. However, the interested reader is invited to find complementary explanations in the following review papers [12–15].

2.1. Bayesian framework and Fisher Information Matrix

Without loss of generality, solving an inverse problem aims at updating the internal parameters $\theta \in \Theta$ of a given model \mathcal{M} from measurements $y \in \mathcal{Y}$ collected under a given loading F . We denote N_s the amount of sensors and N the number of acquired data points. In most SHM applications, measurements are discrete kinematic quantities (displacements, strains, accelerations) that directly derive from the mechanical state predicted by the model $u = \mathcal{M}(\theta, F) \in \mathcal{X}$. The projection operator $\Pi : \mathcal{X} \mapsto \mathcal{Y}$ thus allows to compare explicitly predictions with the available N_s measurements. Classically, measurements are correlated to predictions using the observation equation [18, 21]:

$$y = \Pi(u(\theta)) + w \quad (1)$$

where w is an additive noise assumed to be Gaussian of covariance matrix Σ_w allowing to take into account measurement noise and model discrepancies. In what follows attention is paid to the best choice of sensors locations in order to obtain the best (statistical) identification of θ . Briefly, let us start from the Bayes theorem:

$$\pi(\theta|y) \propto \pi(y|\theta) \cdot \pi_0(\theta) \quad (2)$$

$\pi_0(\theta)$ is the prior probability density function (pdf) on parameters constructed from *a priori* knowledge. $\pi(\theta|y)$ is the posterior pdf; this conditional probability is the final result improved by the knowledge of measured data, reducing uncertainty and giving the most likely values of θ . Finally, $\pi(y|\theta)$ is the so-called likelihood pdf, which can be interpreted as a measure of how good the parametrized model succeeds in explaining the observations. With the previous assumptions, the posterior pdf takes the form:

$$\pi(\theta|y, \Sigma_w) \propto \exp \left[-\frac{1}{2} \mathcal{J}(\theta, y, \Sigma_w) \right] \cdot \pi_0(\theta) \quad \text{with} \quad \mathcal{J}(\theta, y, \Sigma_w) = \sum_{k=1}^N \|\Pi u_k(\theta) - y_k\|_{\Sigma_w^{-1}}^2 \quad (3)$$

where $\|\square\|_{\Sigma_w^{-1}}^2 = \square^T \Sigma_w^{-1} \square$ refers to the squared Euclidean norm of \square weighted by matrix Σ_w^{-1} . \mathcal{J} measures the correlation between measurements and predictions. This functional is also minimized in a deterministic viewpoint to identify optimal parameters (with a complementary regularization to circumvent the ill-posedness of the inverse problem). The sensor placement problem then consists in finding the best projector $\hat{\Pi}$ which minimizes the covariance on the parameter estimate. Note that, because models are numerically discretized (*e.g.* in the finite element sense), then sensors location are optimized among a "grid" of all N_d possible sensor locations. Doing so, the OSP problem becomes a combinatorial optimization problem, that is well-known for being exploratory and computationally expensive.

If the Fisher Information Matrix (FIM), denoted Q , was originally introduced as the inverse of the Cramér-Rao bound (of the parameters covariance matrix) [21], it can also be derived from the statistical viewpoint as the variance of the score, *i.e.* the gradient of the log-likelihood function $\pi(y|\theta)$:

$$Q = \mathbf{E}_\theta \left(\left(\frac{\partial \log \pi(y|\theta)}{\partial \theta} \right) \left(\frac{\partial \log \pi(y|\theta)}{\partial \theta} \right)^T \right) \quad (4)$$

with $\mathbf{E}_\theta(\bullet)$ referring to the mathematical expectation operator on θ . Unsurprisingly, the FIM is strongly related to the sensitivity of predictions with respect to the parameters. It is a relevant mathematical entity on which the sensor selection can rely as it is a way of measuring the amount of information carried by a given sensor configuration. This explains why first OSP works were aiming at maximizing the FIM, in the sense of a certain measure [16, 18–20].

OSP techniques then differ according to the quantity of interest that is considered. Originally, OSP for SHM was focused on modal analysis as damage is related to eigenmodes changes in shape or frequency. A wide spectrum of techniques have been developed, the most popular ones being the effective independence [19, 24, 58–60] and the modeshape difference method [61, 62] that exploit the sensitivity of parameters with respect to eigenmodes. It is also worth mentioning the modal kinetic energy technique that intends to locate sensors at points of maximum modal kinetic energy [63]. Although related to effective independence [64], the modal kinetic energy method is more likely to provide sensor locations in areas where the signal-to-noise ratio should be important, which limits the spurious effects of measurement noise when performing modal analysis.

2.2. Information Entropy

Contrary to the above mentioned techniques that are based on the sensitivity of modal features, one can formulate the OSP problem from the Bayesian viewpoint: the posterior pdf (3) represents the uncertainty of parameters θ based on the information contained in measurements y . The concept of Information Entropy has been introduced to provide a scalar measure of this uncertainty [27, 28]. It benefits from the Bayesian statistical framework as it properly handles measurement uncertainties as well as model errors. The information entropy h is defined as

$$h(\Pi, y) = \mathbf{E}_\theta(-\log \pi(\theta|y)) \quad (5)$$

with $\mathbf{E}_\theta(\bullet)$ referring to the mathematical expectation operator on θ . The information entropy depends on the available data, and the sensor configuration characterized by Π . OSP is then achieved by minimizing the changes in h , which is a unique measure of the uncertainty in the model parameters. A rigorous mathematical description of the information entropy concept for OSP is given in [27, 28] for the case of "small" and "large" uncertainties on the parameters to estimate. A major result that has been shown is the asymptotic result for large amount of available data that relates the information entropy to the determinant of the FIM. Choosing an *a priori* relevant value θ_0 which minimizes the misfit function \mathcal{J} leads to the following approximation when $NN_s \rightarrow \infty$:

$$h(\Pi, y) \approx H(\Pi, y; \theta_0) = \frac{1}{2}N_\theta \log 2\pi - \frac{1}{2} \log \det(Q(\Pi, \theta_0, y)) \quad (6)$$

with $Q(\Pi, \theta_0, y) = NN_s \nabla_\theta \nabla_\theta^T (\mathcal{J}(\theta, y, \Sigma_w)) \approx \sum_{i=1}^N (\Pi \nabla_\theta u_i)^T (\Pi \Sigma_w \Pi^T)^{-1} (\Pi \nabla_\theta u_i)$

where $N_\theta = \dim(\Theta)$ is the number of parameters, N the number of measured samples and N_s the number of sensors. Using (6), one can thus look for N_s optimal sensors locations $\hat{\Pi}$ solving:

$$\hat{\Pi} = \arg \max_{\Pi} [\log \det(Q(\Pi, \theta_0, y))] \quad (7)$$

Even if one may be confident in the relevance of θ_0 to provide effective OSP, this may not be enough when considering strong variations of θ during forthcoming experiments, that may directly impact the structure response, and therefore the FIM. For example, considering the case of complex damageable structures, one may not straightforwardly guess where damage will appear first. This case is referred to as "large" parameter uncertainties in [27]. It implies one

should explore the parameter space (for example with Monte-Carlo sampling) and average the contributions of the FIM computed according to each sample:

$$\hat{\Pi} = \arg \max_{\Pi} \left[\int_{\Theta} \log \det(Q(\Pi, \theta, y)) \pi_0(\theta) d\theta \right] \quad (8)$$

Of course, that type of approach is more expensive from the computational viewpoint, but it is recommended when (i) the initial parameter guess is poorly known, (ii) the updated parameters may strongly vary during experiments, (iii) the sensitivity of Q with respect to θ is significant within the range of likely values of θ .

There have been much use of the information entropy for OSP in the last two decades, especially because it allows to compare sensor configurations of various sizes [65], as one can guess that adding sensors is always beneficial (or at least equivalent) [28], which justifies the relevance of sequential placement strategy compared to genetic algorithms (with much less computational effort). Without being exhaustive, let us mention some significant contributions: in [38], the functional has been extended to take into account the effect of sensors spatial correlation in Σ_w . Similarly, a penalty term to enforce the sparsity of the sensor configuration has been considered in [66]. The information entropy was also used to design optimal loading conditions e for optimal identification [67]. In [37], a multi-objective optimization problem was introduced to design an OSP dedicated to a class of models. Information entropy was applied to statistical seismic source inversion in [68] and to optimal crack identification on plates from strain measurements in [69]. Very recently, the case of multiple damage scenario with modal expansion was considered in [70] to handle virtual sensing under output-only vibration measurements.

Algorithm 1: FSSP algorithm based on information entropy

Initialization:

- Grid of all N_d possible sensors locations
- Targeted number of sensors N_s
- $n = 0$ number of selected sensors
- Set of simulated measurements y

while $n < N_s$ **do**

Consider all possible combinations by adding one new sensor: $\{\Pi_j\}_{j \in \llbracket 1; N_d - n \rrbracket}$

for $j \in \llbracket 1; N_d - n \rrbracket$ **do**

| Evaluate the information entropy of the sensor configuration given by Π_j

end

Identify the sensor configuration $J = \arg \max_{j \in \llbracket 1; N_d - n \rrbracket} [\log \det(Q(\Pi_j, \theta_0, y))]$

Store the new sensor of configuration J as the $(n + 1)^{\text{th}}$ optimal position

end

3. The modified Constitutive Relation Error in dynamics

As explained above, the modified CRE is a model updating functional built as a quadratic data-to-model distance enriched with a term based on the so-called concept of Constitutive Relation Error. It is a credible model updating alternative that has shown its enhanced performance in several applications [39, 40, 47]. The key ingredients for the formulation and minimization of the mCRE in dynamics when updating stiffness parameters are recalled below.

3.1. FE framework, measurements and stiffness parametrization

Let us consider the general case of an elastic structure Ω spatially discretized in E (non-overlapping) finite elements such that $\Omega = \cup_{e=1}^E \Omega_e$ subjected to a given dynamical loading F . We denote by K, D, M the stiffness, damping and mass FE matrices, respectively, while F_ω and

U_ω are the frequency counterparts of nodal loading conditions and displacement field. With these notations, the dynamic equilibrium written in the frequency domain at a given angular frequency ω reads:

$$[-\omega^2 M + i\omega D + K] U_\omega = F_\omega \quad (9)$$

In addition, a set of sensors is used to measure the magnitude of some kinematic quantities (displacement, velocity and/or accelerations). In the frequency domain, assuming measurements are perfect, such information can be written without loss of generality as:

$$\Pi U_\omega = Y_\omega \quad (10)$$

where Y_ω refers to the frequency counterpart of measurements at angular frequency ω , and Π contains zero and integer powers of $i\omega$ to extract displacement field derivatives at corresponding sensors positions.

As the main driver of this report is to perform SHM and damage detection, one can (legitimately) assume that damage can be interpreted as local stiffness loss. Therefore, a convenient manner to parametrize a linear FE problem for damage detection is to parametrize the FE stiffness matrix. The latter is thus decomposed in N_θ non-overlapping subdomains and parametrized as follows:

$$K(\theta) = \sum_{i=1}^{N_\theta} \theta_i K_{0,i} \quad \text{with} \quad K(\theta_0) = \sum_{i=1}^{N_\theta} K_{0,i} \quad \text{and} \quad \theta \in \Theta \subset \mathbb{R}^{N_\theta} \quad (11)$$

Note that the subdomains can perfectly match with finite elements or gather some of them to reduce the number N_θ of parameters to identify.

3.2. mCRE-based model updating problem in dynamics

Contrary to standard deterministic approaches, the fundamental idea of mCRE-based model updating is to built mechanical fields and to identify structural parameters simultaneously as a trade-off according to all available information (*i.e.*, physics knowledge and measured data). Therefore, there is no need for additional *a priori* information. The starting point of the approach thus consists in classifying, among the data and equations of the mechanical problem, what will be considered as 'reliable' from what should be considered with caution (labelled 'unreliable'). This separation is non-unique and deeply relies on the case study and engineering expertise, although it is also well-known that constitutive relations are (very often) the less reliable equations. The separation of equations for the considered case is given in TAB. 1. Doing so, we define two manifolds: (i) \mathcal{U}_{ad} the so-called kinematically admissible space that contains the FE displacement fields satisfying the boundary conditions and kinematic relations but not necessarily the constitutive equations, and (ii) \mathcal{D}_{ad} the so-called dynamically admissible space containing the FE displacement fields V such that $[-\omega^2 M + i\omega D]U + K(\theta)V = F_\omega$ for all $U \in \mathcal{U}_{ad}$. In other words, \mathcal{D}_{ad} contains the displacement fields satisfying both equilibrium and constitutive equations. The reciprocity gap between those two manifolds can be measured using an energy norm - the CRE - that estimates the relevance of a solution couple $s_\omega = (U_\omega, V_\omega) \in \mathcal{U}_{ad} \times \mathcal{D}_{ad}$ with respect to the mechanical problem. With the above notations, the CRE at a given angular frequency ω reads:

$$\zeta_\omega^2(s_\omega, \theta) = \frac{1}{2}(U_\omega - V_\omega)^H K(\theta)(U_\omega - V_\omega) = \frac{1}{2}\|U_\omega - V_\omega\|_{K(\theta)}^2 \quad (12)$$

The extension of the CRE concept to unreliable experimental data (see TAB. 1) directly leads to the so-called *modified Constitutive Relation Error* (mCRE). In the latter, the CRE is extended with a data-to-model distance written in the frequency domain:

$$e_\omega^2(s_\omega, \theta, Y_\omega) \triangleq \zeta_\omega^2(s_\omega, \theta) + \alpha \frac{1}{2}\|\Pi U_\omega - Y_\omega\|_G^2 \quad (13)$$

	Reliable	Unreliable
Model	<ul style="list-style-type: none"> • Geometry • Boundary conditions • Equilibrium equations • Dissipative constitutive relations 	<ul style="list-style-type: none"> • Elastic constitutive relations
Experiments	<ul style="list-style-type: none"> • Loading frequencies $\omega/2\pi$ • Sensors locations • Measured inputs F_ω 	<ul style="list-style-type: none"> • Measured outputs Y_ω

TABLE 1: Distinction between reliable and unreliable information for damage detection from stiffness update in dynamics.

α is the confidence into measurement scaling parameter, allowing to give more or less importance to the measurements in the model updating process (particularly regarding the noise level). Its calibration is crucial to obtain relevant mCRE-based model updating results [47]. G is a symmetric positive-definite matrix that guarantees that $\|\square\|_G$ is homogeneous to ζ_ω^2 and equivalent in level. Its choice is much less critical than α . In practice, G is chosen as proportional to the identity matrix and weighted by the first eigenvalue of $K(\theta_0)$.

Finally, the analysis of a single angular frequency may be too restrictive in dynamics, particularly when several eigenmodes are simultaneously excited. The full mCRE functional \mathcal{J} to be minimized is thus obtained by direct integration over a frequency bandwidth D_ω (which stores the essential information about the structure response):

$$\mathcal{J}(\theta, Y) = \int_{D_\omega} z(\omega) e_\omega^2(\hat{s}(\theta, Y_\omega), \theta, Y_\omega) d\omega \quad (14)$$

where $z(\omega)$ is a frequency weighting normalized function such that $\int_{D_\omega} z(\omega) d\omega = 1$ allowing to modulate the importance of specific frequencies of D_ω and \hat{s} the optimal mechanical fields for a given parameter set and given measurements. In the present formulation of the mCRE in the frequency domain, \hat{s} at each angular frequency ω is obtained solving:

$$\forall \omega \in D_\omega, \quad \hat{s}_\omega(\theta, Y_\omega) = (\hat{U}_\omega, \hat{V}_\omega) = \arg \min_{s \in (\mathcal{U}_{ad} \times \mathcal{D}_{ad})} e_\omega^2(s, \theta, Y) \quad (15)$$

which is a minimization problem constrained by the satisfaction of the dynamic equilibrium between the manifolds \mathcal{U}_{ad} and \mathcal{D}_{ad} . In practice, an augmented cost-function with Lagrange multipliers is introduced, which leads to the matrix system written below that must be solved for all ω in D_ω (see [47, 53] for further details):

$$A \begin{bmatrix} \hat{U}_\omega - \hat{V}_\omega \\ \hat{U}_\omega \end{bmatrix} = b \text{ with } \begin{cases} A &= \begin{bmatrix} [K(\theta) + i\omega D - \omega^2 M]^H & \alpha \Pi^H G \Pi \\ -K(\theta) & [K(\theta) + i\omega D - \omega^2 M] \end{bmatrix} \\ b &= \begin{bmatrix} \alpha \Pi^H G Y_\omega \\ F_\omega \end{bmatrix} \end{cases} \quad (16)$$

The overall mCRE-based model updating problem thus reads:

$$\hat{\theta} = \arg \min_{\theta \in \Theta} \left\{ \mathcal{J}(\theta, Y) \triangleq \int_{D_\omega} z(\omega) e_\omega^2 \left(\left[\arg \min_{s \in \mathcal{U}_{ad} \times \mathcal{D}_{ad}} e_\omega^2(s, \theta, Y_\omega) \right], \theta, Y_\omega \right) d\omega \right\} \quad (17)$$

3.3. Additional remarks

Although the nested minimization problem (17) on mechanical state and parameters make the algorithmic structure for minimization quite complex compared to classical model updating

methods, one should notice that the computation of mechanical fields for a given value of θ is not computationally expensive as the size of (16) can be drastically reduced using projection on reduced truncated modal basis [71].

The minimization of the mCRE with respect to parameters can be numerically performed using unconstrained minimization algorithms such as the BFGS algorithm. With the analytical expression of the gradient of the mCRE with respect to parameters (see Appendix A), the computational burden associated to the minimization process is reduced. These expressions are also decisive in the following to improve the numerical performance of the mCRE-based OSP.

If supplying an analytical Hessian matrix may lead to minor computational improvements when minimizing the mCRE, it can still be exploited to compute confidence intervals [53]. Indeed, when identifying several parameters simultaneously, one could wonder what relative precision is reached in the identification process for uncertainty quantification. To do so, one can thus consider the computation of confidence intervals as a first approach. More details are given in Appendix B.

Lastly, note that the relevant frequency range for earthquake engineering problems is below 50 Hz, which justifies the frequency-domain formulation dedicated to low-frequency dynamics presented in this paper. The forthcoming OSP framework can still be extended if needed to other types of loading conditions using the time-domain formulation of the mCRE [72].

4. A mCRE-oriented OSP strategy

For structures having heterogeneous sensitivity of stiffness to model updating, parameter estimates may be quite far from reality when the model updating process is performed using a small amount of sensors. This is the case for several SHM applications considering one cannot always afford for rich instrumentation on large scale structures. If OSP strategies have been proposed for (standard) structural identification and modal analysis, there is no proper sensor placement strategy dedicated to mCRE-based model updating in the literature whereas it has shown to be an efficient alternative to standard approaches [39]. In the following, we present a modified FIM that integrates the mCRE concept, which is warranted in light of the link between the mCRE (though deterministic) and the Bayesian inference framework for Gaussian random variables.

4.1. Interpretation of the mCRE from a Bayesian viewpoint

Although the previously introduced mCRE-based model updating strategy is deterministic, one can show that this procedure is equivalent to the Maximum *A Posteriori* (MAP) estimation in the Bayesian inference framework with Gaussian distributions, an error norm based on the measurement error covariance matrix, and no *a priori* on parameters [73, 74]. Since covariance on the modeling error is usually not known, the idea is to integrate modeling error in a different manner into Bayesian inference, in a more global and less strict framework that allows more flexibility in the model structure.

If one assumes that the prior pdf $\pi_0(\theta)$ and the likelihood function $\pi(y|\theta)$ are both defined with Gaussian distributions, then

$$\pi_0(\theta) \propto \exp \left[-\frac{1}{2} (\theta - \bar{\theta})^T \Sigma_0^{-1} (\theta - \bar{\theta}) \right] \quad (18)$$

$$\pi(y|\theta) \propto \exp \left[-\frac{1}{2} (\Pi(\mathcal{M}(\theta, e)) - y)^T [\Sigma_m + \Sigma_y]^{-1} (\Pi(\mathcal{M}(\theta, e)) - y) \right] \quad (19)$$

where $\Sigma_0, \Sigma_m, \Sigma_y$ respectively denote the *a priori*, model and observations covariance matrices. $\bar{\theta}$ is the mean of the prior pdf. Therefore, according to the Bayes theorem (2) and the MAP

principle, the optimal set of parameters can be sought as

$$\begin{aligned} \hat{\theta} &= \arg \max_{\theta \in \Theta} \pi(\theta|y) = \arg \max_{\theta \in \Theta} \pi(y|\theta) \cdot \pi_0(\theta) \\ &= \arg \min_{\theta \in \Theta} \left[\underbrace{(\Pi(\mathcal{M}(\theta, e)) - y)^T [\Sigma_m + \Sigma_y]^{-1} (\Pi(\mathcal{M}(\theta, e)) - y)}_{\text{Least-square term (Mahalanobis distance)}} + \underbrace{(\theta - \bar{\theta})^T \Sigma_0^{-1} (\theta - \bar{\theta})}_{\text{Regularization term}} \right] \end{aligned} \quad (20)$$

This way, the structure of the constitutive relation is imposed strongly, and it is assumed to know the modeling error features, which is not the case in most problems. To avoid this issue, the mCRE strategy integrates modeling error in a global manner that allows for more flexibility in the model structure. To the modeling error (the CRE) is thus associated a pdf to globally quantify the confidence on the less reliable parts of the model:

$$\pi_{CRE} \propto \exp \left[\frac{-1}{\alpha} \zeta^2(s, \theta) \right] \quad (21)$$

The confidence on the modeling exponentially decreases when the CRE value increases, with a rate speed specified by the scalar α . Therefore, in a mCRE context with a measurement error norm based on the covariance of the measurements Σ_y , one can rewrite the likelihood pdf:

$$\pi(y|\theta) \propto \exp \left[-\frac{1}{2} (\Pi(\mathcal{M}(\theta, e)) - y)^T \Sigma_y^{-1} (\Pi(\mathcal{M}(\theta, e)) - y) \right] \cdot \exp \left[\frac{-1}{\alpha} \zeta^2(s, \theta) \right] \quad (22)$$

for any admissible mechanical solution s . Thus, if one no longer assumes any a priori on θ (uniform pdf), the application of the MAP principle leads to:

$$\hat{\theta} = \arg \min_{\theta \in \Theta} \left[(\Pi(\mathcal{M}(\theta, e)) - y)^T \Sigma_y^{-1} (\Pi(\mathcal{M}(\theta, e)) - y) + \frac{1}{\alpha} \zeta^2(s, \theta) \right] \quad (23)$$

where one easily recognizes the sum of a model error (the CRE) with a data-to-model distance to minimize. It thus illustrates, although the mCRE remains a deterministic functional, its metric can be closely related to the Bayesian inference framework in the case of Gaussian random variables.

4.2. mCRE-based OSP: modified Fisher Information Matrix

The key idea of the proposed sensor placement technique is to use the mechanical fields $\{U_\omega\}_{\omega \in D_\omega}$ computed for mCRE needs within the Information Entropy concept. Mathematically, we thus define a modified Fisher Information Matrix Q_m such that:

$$Q_m = \sum_{\omega \in D_\omega} (\Pi \nabla_\theta U_\omega)^T (\Pi \Sigma_y \Pi^T)^{-1} (\Pi \nabla_\theta U_\omega) \quad (24)$$

In other words, the modified FIM analyzes the sensitivity of the mCRE measurement error part with respect to the parameters to identify. The effect of the CRE is implicit in the computation of U_ω . Similarly to former OSP techniques, the determinant of the modified FIM is maximized to optimally position sensors (assuming the amount of data is large enough to reuse the asymptotic result mentioned above). Although all the previously mentioned sensor placement algorithmic structures are applicable (as only the FIM definition is changed), ALG. 2 presents the mCRE-based OSP algorithm in a FSSP framework for direct comparison with ALG. 1.

It is worth noticing that the access to a semi-analytical expression of the gradient of U_ω with respect to θ is a valuable asset to perform OSP in reasonable CPU times: the modified FIM Q_m can thus be computed quickly without any loss of precision. One should notice that the computation of $\nabla_\theta U_\omega$ is a low-cost post-processing operation once (16) has been solved (see Appendix A for mathematical developments).

Algorithm 2: mCRE-based FSSP algorithm

Initialization:

- Grid of all N_d possible sensors locations
- Targeted number of sensors N_s
- Number of selected sensors $n = 0$
- Initial parameter guess $\theta_0 \in \Theta$
- Set of simulated measurements y (obtained with θ_0)
- FE model including mesh and matrices K, D, M
- mCRE tuning parameters: frequency bandwidth D_ω , confidence into measurements scalar α , frequency weighting function $z(\omega)$

while $n < N_s$ **do**

 Consider all possible combinations by adding one new sensor: $\{\Pi_j\}_{j \in \llbracket 1; N_d - n \rrbracket}$
for $j \in \llbracket 1; N_d - n \rrbracket$ **do**

 Initialize the modified FIM $Q_{m,j} = 0$
for $\omega \in D_\omega$ **do**

 Get mechanical fields (U_ω, V_ω) solving the $AX = b$ system (equation 16)

 Compute $\nabla_\theta U_\omega$ (equation 39)

 $Q_{m,j} = Q_{m,j} + (\Pi_j \nabla_\theta U_\omega)^T (\Pi_j \Sigma_y \Pi_j^T)^{-1} (\Pi_j \nabla_\theta U_\omega)$
end
end

 Identify the sensor configuration $J = \arg \max_{j \in \llbracket 1; N_d - n \rrbracket} \{\det(Q_{m,j})\}$

 Store the new sensor of configuration J as the $(n + 1)^{th}$ optimal position

 Go to the next iteration: $n \rightarrow n + 1$
end

5. Application to accelerometer optimal placement for damage detection

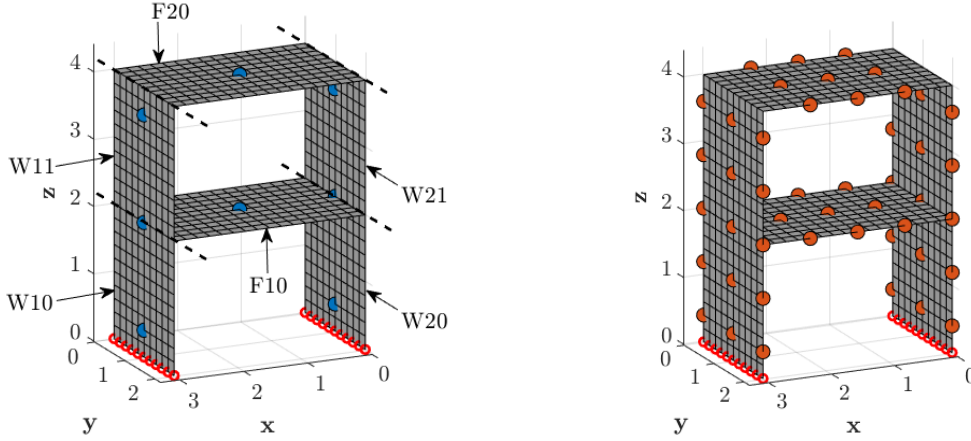
5.1. Description of the problem

345 We aim to present the benefits of mCRE-based OSP for mCRE-based model updating in a case study whose geometry and loading conditions are representative of earthquake engineering problems. Inspired from the SMART2013 test campaign that has been recently used for mCRE applications [47, 75], we consider the two-story frame structure of FIG. 1 submitted to a tridimensional low-magnitude random ground acceleration. Such input signals are used
 350 in earthquake engineering experiments to perform modal identification [76] once damage has occurred. The objective of this study is to position at best a restricted budget of accelerometers in order to identify accurately the uncertain stiffness distribution of the structure in forthcoming (possibly damaging) experiments. As we assume that very few sensors are available, an intuitive coarse stiffness parametrization of the stiffness is proposed: 6 subdomains are defined {W10,
 355 W11, W20, W21, F10, F20}, one per wall and per slab. The updated stiffness model (11) is thus made of $N_\theta = 6$ parameters. The subdomains areas are shown in FIG. 1. The model is made of shell elements using the CEA modeling software CAST3M[©] [77]. Relative time acceleration measurements in both x and y directions are simulated using Fast Fourier Transforms and the direct dynamics problem formulated in terms of relative displacement is:

$$M\ddot{x} + D\dot{x} + K(\theta)x(t) = -M\Xi\ddot{u}_d, \quad x = u - u_d \quad (25)$$

360 where Ξ is a matrix addressing the acceleration ground motion to the associated dofs and \ddot{u}_d the random ground acceleration input constructed as a multivariate zero-mean Gaussian process.

The objective of this application is to assess the proposed sensor placement strategy for efficient mCRE-based identification. To restrain CPU times and avoid sensors concentrations, we define a grid on 48 potential sensor locations: a triaxial accelerometer can be positioned at
 365 each orange dof of FIG. 1.



(a) Frame with uniform sensor placement (blue dots).

(b) Grid of possible accelerometer locations.

FIGURE 1: Frame structure - uniform default sensor placement and grid of possible locations for OSP. Subdomains areas and denomination are also given.

Although several types of sensors could be positioned simultaneously, only accelerometers are considered herein because they are a popular, minimally invasive and easily deployable sensing devices for SHM and earthquake engineering applications. In order to be realistic regarding what could be achieved in practical shaking table tests, a restricted budget of $N_s = 24$ data acquisition channels has been fixed. $N_s = 24$ allows to uniformly spread enough sensors to reproduce typical sensor placement configurations that are done in earthquake engineering applications. Besides, as $N_\theta = 6$ parameters are supposed to be updated, it is theoretically enough to get proper identification results and redundancy in the information carried out by measurements.

5.2. OSP benchmark

In order to assess the relevance of mCRE-based OSP with respect to other OSP strategies, a numerical benchmark has been conducted to perform and compare sensor placements oriented towards different quantities of interest. An overview of the tested strategies is presented in TAB. 2. OSP algorithms for modal analysis (MA# case), structural identification (SI# cases) and mCRE-based model-updating are compared, for uniaxial and triaxial accelerometers. The case of multiple scenarios is also considered for mCRE-based OSP (mCRE-MS# cases). A FSSP optimization algorithm is used in all cases to fairly compare sensor placement results between methods. As a reminder, FSSP and genetic algorithms have similar performance when the number of sensors to position remains small [28].

Description and designation		Optimality criterion	Accelerometer type
Reference richest OSP ($N_s = 48$)	Ref	-	-
Uniform default OSP	Def	-	Triaxial
OSP for modal analysis of the 10 first structural eigenmodes	MA1	$\log(\det Q(\Phi))$	Uniaxial
	MA2		Triaxial
OSP for standard structural identification	SI1	$\log(\det Q(X))$	Uniaxial
	SI2		Triaxial
mCRE-based OSP	mCRE1	$\log(\det Q_m)$	Uniaxial
	mCRE2		Triaxial
mCRE-based OSP for uncertain damage scenarios	mCRE-MS1	$\int_{\Theta} \log(\det Q_m) \pi_0(\theta) d\theta$	Uniaxial
	mCRE-MS2		Triaxial

TABLE 2: OSP benchmark

Among the proposed sensor placement strategies, it should be highlighted that:

385

▷ In the reference richest OSP, all the possible locations are covered with triaxial accelerometers, meaning $N_s = 48$ in that case. This is not a realistic configuration, neither an economical one, but it allows to provide results that will be used as reference when comparing the performance of OSPs in terms of model updating.

390

▷ In the uniform default case, 8 triaxial accelerometers are uniformly spread over the structure. This is typically what should be done naively without considering OSP algorithms in practice.

395

▷ Optimal uniaxial and triaxial accelerometer placement are systematically compared. Of course, positioning triaxial sensors is much more convenient from the experimental viewpoint, as it is less constraining for the instrumentalists. Besides, it is less computationally demanding than uniaxial accelerometer placement because the number of possible sensor configurations is reduced. However, forcing triaxial sensors implies the addition of constraints to OSP strategies, which should thus lead to less performant results as less freedom is given to the sensor plan.

400

▷ The OSP strategies oriented towards modal analysis aim at identifying at best the 10 first structural eigenmodes. The latter are stored in the modeshape matrix Φ , and the associated FIM reads:

$$Q(\Phi) = (\Pi\Phi)^T (\Pi\Sigma_y\Pi^T)^{-1} (\Pi\Phi) \quad (26)$$

405

which is independent of the nominal stiffness parameter values θ_0 . In addition, the optimal sensor locations are also independent of the excitation used. The FIM in that case has exactly the same form as the one proposed for the effective independence method [19]. Finally, as 10 modes are stored in Φ , one should expect to get singular FIM while less than 10 sensors have not been positioned on the specimen. To avoid numerical issues, the determinant of the FIM will be computed as the product of the non-zero eigenvalues of $Q(\Phi)$.

410

▷ The OSP for structural identification directly deals with the identification (in a least-square sense) of the stiffness parameters. In that case, the FIM is directly computed from the sensitivity of the frequency-domain counterpart of the mechanical state X with respect to the parameter set θ :

$$Q(X) = \sum_{\omega \in D_\omega} (\Pi\nabla_\theta X_\omega)^T (\Pi\Sigma_y\Pi^T)^{-1} (\Pi\nabla_\theta X_\omega) \quad (27)$$

with (for the considered stiffness parametrization):

$$\nabla_\theta X_\omega = - [-\omega^2 M + i\omega D + K(\theta)]^{-1} \frac{\partial K}{\partial \theta} [-\omega^2 M + i\omega D + K(\theta)]^{-1} [\omega^2 M \Xi U_{d,\omega}] \quad (28)$$

415

For legitimate comparisons with mCRE-based OSP, the frequency range that is considered to compute $Q(X)$ is also D_ω . Note that the FIM could also be obtained with time-domain measurements, but the sensitivity matrix would be computed by solving a (more expensive) full time domain problem [38].

420

Contrary to the MA cases, the optimal sensor locations depend on the location and type of excitation that is used. Also, the matrix $Q(X)$ may be non-singular even for only one positioned sensor since the structural response obtained from the model may store enough information from all contributing eigenmodes in order to estimate the parameter set θ .

▷ Regarding the settings of the mCRE, as the first five modes of the structure are below 20 Hz and are the most sollicitated ones, a frequency bandwidth $D_\omega = [1 \text{ Hz}; 30 \text{ Hz}]$ with $\Delta f = 0.1 \text{ Hz}$ has been chosen for the computation of all forthcoming results. The call

425

to a reduced basis made of the first 20 eigenmodes of the frame allows to achieve fast and accurate mCRE computations as it largely covers the frequency range of interest. The weighting function $z(\omega)$ is computed using the complex modal indicator function as explained in [78]. α will be subject to calibration tests, therefore its value will be specified afterwards.

430

▷ Because one also intends to provide sensor placements that are still efficient once damage has occurred, the case of multiple scenarios mCRE-based optimal sensor placement has been addressed. Following the subdomain decomposition shown in FIG. 1, the 6 parameters have been pseudo-randomly sampled using a Latin Hypercube algorithm in order to take into consideration 30 damage scenarios, assuming the parameter set follows a multivariate uniform pdf on $[0.2;1]$. A uniform prior pdf has been chosen due to the fact it is the less informative in the sense of the statistical maximum entropy. The generated set of samples is denoted Θ_s . Each $\theta_s \in \Theta_s$ is thus used to simulate a dataset y_s , which will be processed to perform OSP. The stiffness parametrization of each scenario is given in FIG. 2. The change on stiffness parameters has significant effects on the frequency domain response of the structure as one can observe in FIG. 3 where the normalized H-CMIF plot for each considered damage configuration is given [47]. The latter is defined as the dominant singular value of the transfer function from the crossed input/output PSD matrices. It is called H-CMIF because of its similarities with the Complex Modal Identification Function [79]. The frequency shift of the H-CMIF peaks shows how the structural response varies from one scenario to the other.

435

440

445

Following the work initiated in [27] for the case of highly uncertain parameters, the optimality criterion is thus approximated by:

$$\int_{\Theta} \log(\det(Q_m(\Pi, \theta, y))) \pi(\theta) d\theta \approx \frac{1}{\text{card}(\Theta_s)} \sum_{\theta_s \in \Theta_s} \log(\det(Q_m(\Pi, \theta_s, y_s(\theta_s)))) \quad (29)$$

450

leading to an optimal sensor placement that is dedicated to a wider range of damage configurations. In practice, it is true that cases involving damage at the top of the structure are highly unlikely, but the uncertainty on parameters provided by this approach enables to take modeling bias into consideration. As a last remark, although not considered here because of the assumed non-damaging nature of the input signals, the variability of loading conditions may also have been exploited if nonlinear damaging models were used, so that the damage scenarios that are generated for OSP are much more realistic.

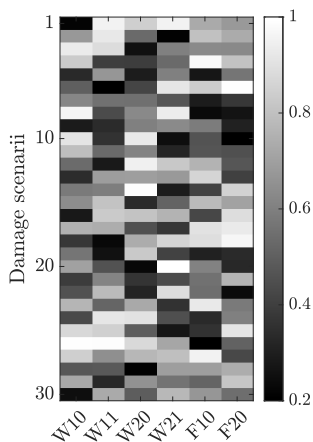


FIGURE 2: Stiffness samples Θ_s to simulate multiple damage scenarios.

455

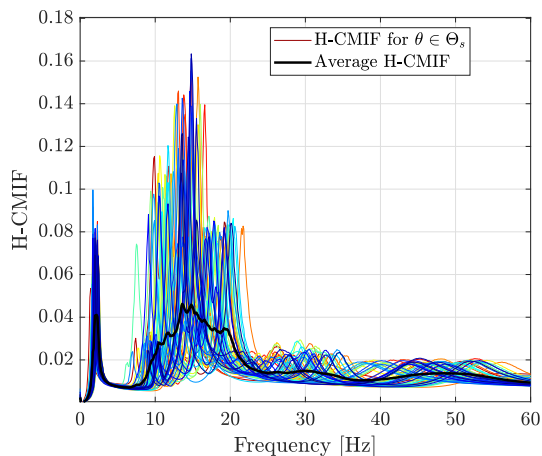


FIGURE 3: Impact of damage configuration on the frequency response of the structure. A wide variability of responses is integrated into the OSP framework.

5.3. OSP results - first comments

5.3.1. Modal identification

The OSP results obtained for modal analysis using a truncated modal basis made of the first 10 modes of the frame are presented in FIG. 4. To confirm the soundness of the results, we plot both $\det(Q)$ and the CMIF obtained after having positioned accelerometers with comparison to the one obtained with the rich OSP configuration.

The amount of information carried by the first sensors is more important as it allows the identification of one supplementary mode. When as many sensors as modes in Φ have been positioned, the additional information carried by new sensors is less important as it only comforts the modal identification, making it more accurate. Due to the complexity of the structure, no clear visual trend from the sensor position can be easily guessed, except that most sensors are located on the floors. This appears to be quite natural as floor eigenmodes are part of the 10 first ones of the structure.

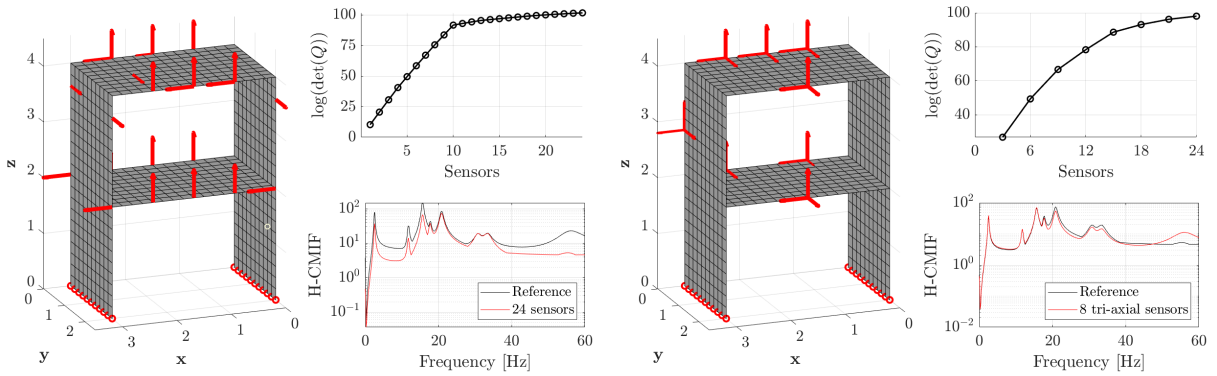


FIGURE 4: OSP of uniaxial and triaxial accelerometers for the MA1 (left) and MA2 cases (right). Accelerometers positions and orientations are given by the red arrows, while determinant of the FIM (in log scale) and H-CMIF are plotted to confirm the soundness of the approach.

5.4. Structural identification OSP results

The OSP results obtained for SI1 and SI2 cases are presented in FIG. 5. The evolution of $\det(Q(X))$ is also given to confirm the relevance of the results. Due to the large parameters sensitivity, the sensor placement is not visually intuitive in the sense that not all subdomains are covered by at least one sensor. One can interpret the fact that sensors are mostly located at the top of the structure because it remains the most kinematically responsive part of the latter. However, from the sudden slope change of the determinant of the FIM with positioned sensors, we find that after the placement of 6 sensors, the system is a priori totally identifiable, meaning that new sensors bring (mostly) redundant information. As a remark, note that the values of $\det(Q(X))$ between the modal analysis OSP and structural identification OSP are not comparable as the FIM definition is different.

5.4.1. mCRE-based OSP results

The OSP results obtained for mCRE1 and mCRE2 cases are presented in FIG. 6. To understand at best the sensor placement process, a particular attention was paid to the sequential positioning of sensors by coloring the sensor position according to their order of appearance in the FSSP algorithm. The value of the $\det(Q_m)$ is also provided. The mCRE settings that allowed to provide the following results are given above. The value of α is well-known to be crucial in the mCRE framework, and as it is not properly tunable at the experimental design stage, its influence on mCRE-based OSP results was explicitly studied. What can be observed

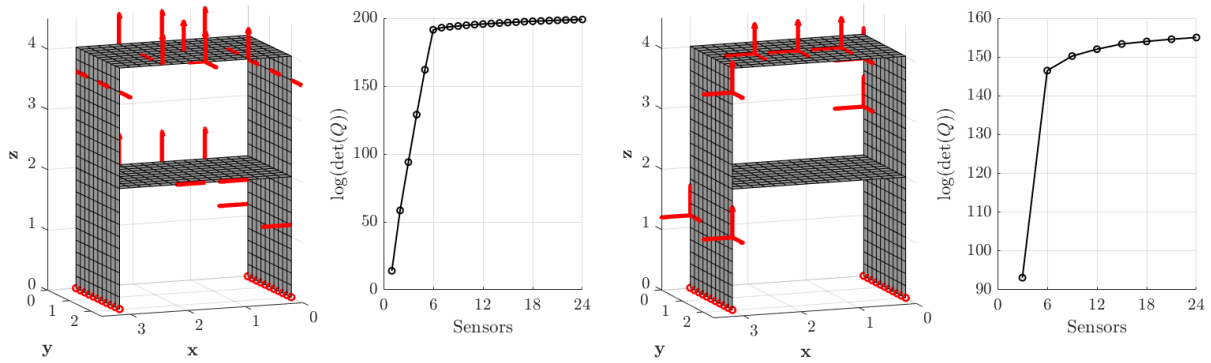


FIGURE 5: OSP of uniaxial and triaxial accelerometers for the SI1 (left) and SI2 cases (right). Accelerometers positions and orientations are given by the red arrows, and the determinant of the FIM (in log scale) is plotted to confirm the soundness of the approach.

at first glance is that the more important the confidence into measurements α , the closer to the bottom of the structure for sensor locations. If the increasing value of $\det(Q_m)$ confirms FSSP behaves correctly, the values plotted in FIG. 6 are not comparable as they are function of α . For the following studies, the confidence into measurements coefficient has been chosen at $\alpha = 10^4$ because of the correct dispersion of the sensors on the whole structure (see FIG. 6).

Finally, OSP results for mCRE-based sensor placement taking multiple damage scenarios into account are presented in FIG. 7. Several remarks can be made from these placements. First, there is no sensor positioned in the x direction for the mCRE-MS1 case, which can explain why the mCRE-MS2 sensor placement is much less optimal in the sense of the criterion to maximize. Unsurprisingly, it is interesting to notice that the first sensors in both cases are located at the bottom of the structure, where damage is most likely to occur. Similarly, few sensors are located on the top walls as they are less identifiable (in the CRE sense) and less prone to damage. Of course, the numerical resources that are necessary to compute these results are much more important, as it requires $\text{card}(\Theta_s)$ times more solutions of the mCRE system. Hopefully the required CPU time did not exceed more than 12 hours on a personal laptop. This numerical effort should be worthwhile, as the resulting sensor placement will be effective over a wider range of stiffness configurations.

5.5. Assessment of sensor configurations for mCRE-based model updating

5.5.1. Model updating contexts

Because we look for optimal sensor placement in the sense of damage detection, we propose to challenge the different OSP that have been obtained and presented previously for mCRE-based model updating using three datasets that fairly represent the typical situations one can meet in practice:

- (i) Updating the model from the same data that has been used to perform OSP. The expected parameter vector is exactly the one that has been used to position sensors.
- (ii) Updating the model from data obtained after an overall 10% stiffness underestimation. This is a situation that can be encountered if model bias is present. Measurements include in that case additional noise for which ratio of standard deviation with input standard deviation is 10%.
- (iii) Updating the model from data obtained in a new damaged scenario. The expected parameter vector is $\theta^* = [0.5 \ 0.9 \ 0.6 \ 0.9 \ 0.8 \ 1]$. Measurements are also polluted with noise (10% in level too).

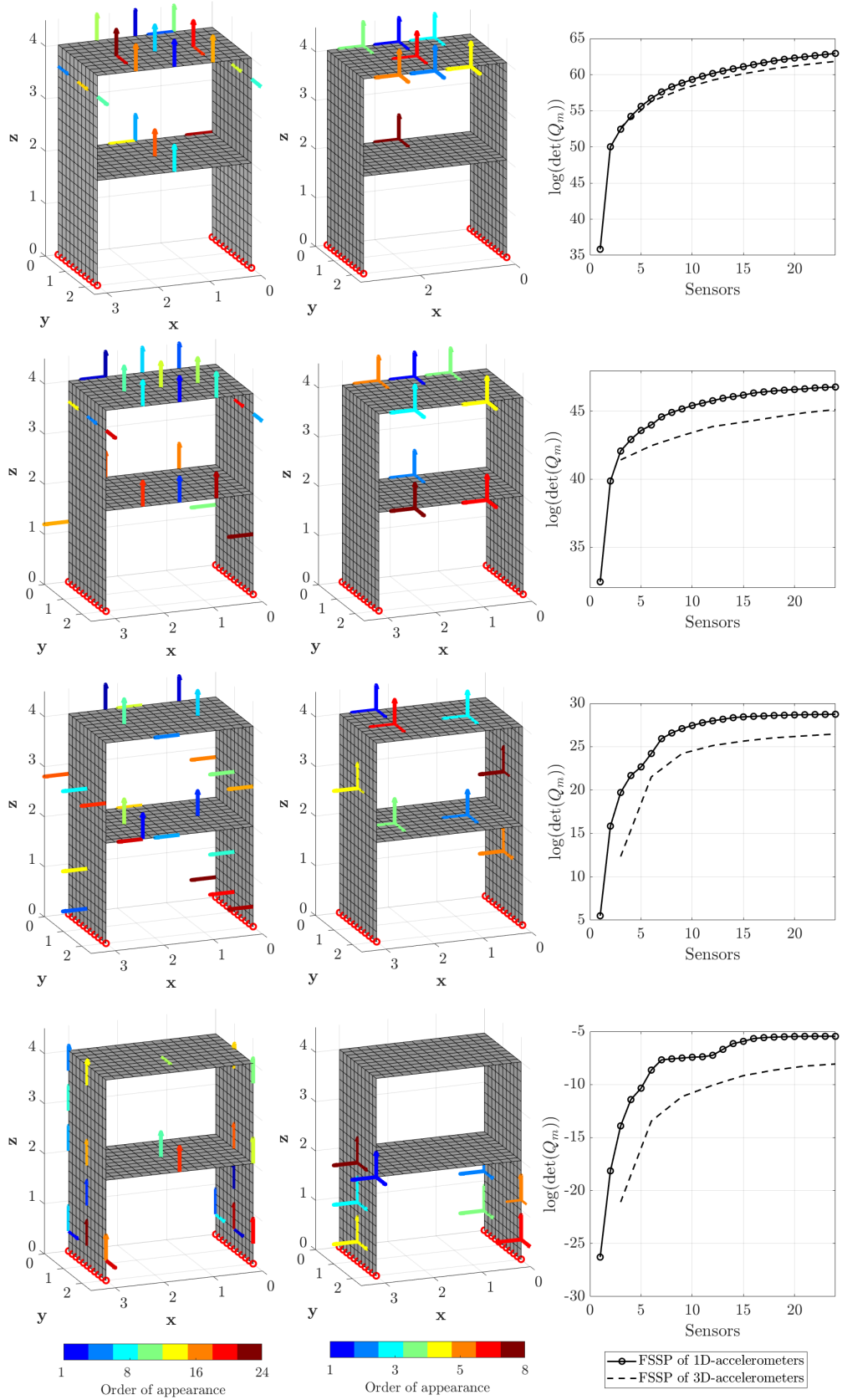


FIGURE 6: mCRE-based OSP of uniaxial and triaxial accelerometers for the identification of the 6-subdomain parametrization of the frame. The arrows indicate the sensor position and their color indicates their order of appearance in the FSSP strategy. From top to bottom, results have been obtained with $\alpha = \{1; 10^2; 10^4; 10^6\}$.

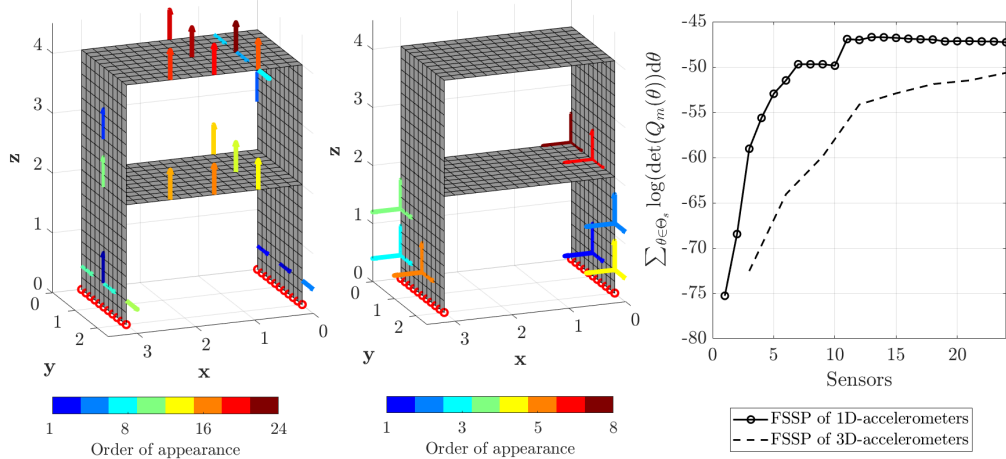


FIGURE 7: mCRE-based OSP of uniaxial and triaxial accelerometers taking multiple damage scenarios into account. The arrows indicate the sensor position and their color indicates their order of appearance in the FSSP strategy. A value of $\alpha = 10^4$ was chosen.

520 Case (i) is probably the most comfortable model updating situation with high-quality measurements; Case (ii) gets more difficult as noise is added to measurements and a uniform model bias must be recovered; Case (iii) is the most challenging problem as a damaged configuration must be identified from noisy measurements using sensors whose positions have been optimized from a totally different parameter estimate (except for mCRE-MS1 and mCRE-MS2 cases). Because of the random nature of measurement noise, one cannot expect to properly assess model updating performance exclusively with parameters estimates. Model updating results will thus be assessed using both parameter estimates and relative confidence intervals widths, using the richest sensor placement as reference.

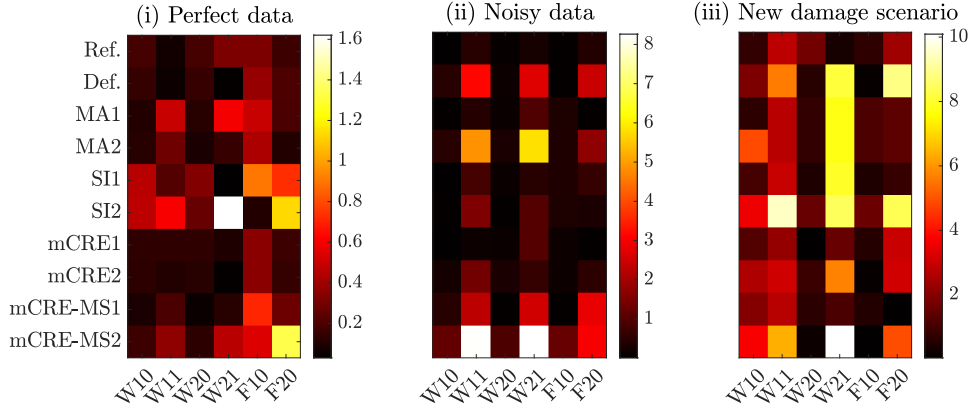
530 The assessment of OSP for model updating is summarized in FIG. 8 with 6 colormaps. For each model updating scenario, we propose two colormaps: the first one indicates the relative gap in [%] of parameter estimates with respect to the exact parameter set that should have been recovered θ^* (see FIG. 8.a). The second one shows the relative width in [%] of confidence intervals with respect to the ones given by the reference sensor placement configuration (see FIG. 8.b and Appendix B for mathematical details).

535 For all maps, each line indicates the performance obtained by a given sensor placement (denominations are given in TAB. 2) while each column corresponds to a given subdomain (denominations are given in FIG. 1).

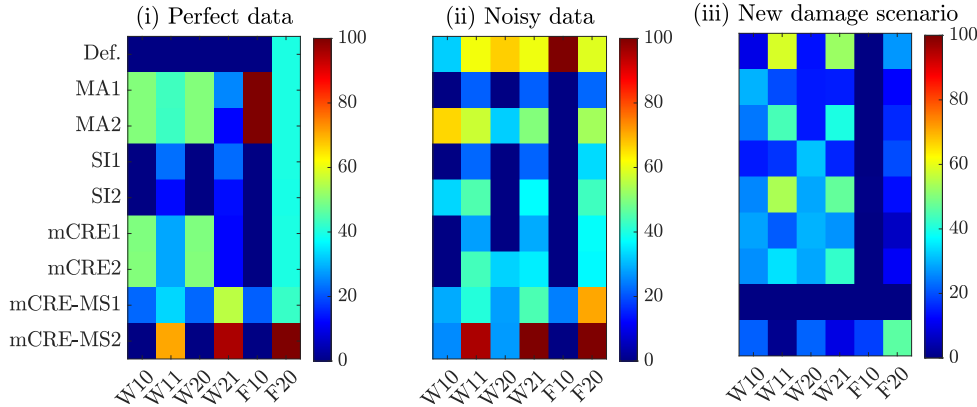
540 The understanding of results displayed in FIG. 8.b is not direct and is recalled in the following lines: a close-to-zero value means that the convexity of the mCRE functional evaluated around $\hat{\theta}$ with a given OSP is almost the same as the one of the mCRE evaluated with the reference sensor placement case in which twice the number of sensors are present. It suggests that the considered sensor placement is efficient in the sense that there is not much additional doubt regarding the value of parameter estimate. On the contrary, when the relative gap on confidence intervals width is important, the mCRE functional is less convex around $\hat{\theta}$, meaning that another measurement noise realization may have lead to significantly different model updating results.

5.5.2. Discussion on the relevance of the modified FIM

550 Several conclusions can be drawn from the results shown in FIG. 8. First, because the number of sensors ($N_s = 24$) was sufficiently important with respect to the number of parameters to be identified ($N_\theta = 6$), correct mCRE-based model updating results have been obtained in all cases as parameters have been correctly identified with less than 10% error with respect to the expected values in the most unfavorable case. The comparison of the maps (a.i) and (a.ii) reveals



(a) Relative gaps on parameter estimates (in [%]) obtained with the different sensor configurations.



(b) Relative gaps on confidence intervals (in [%]) obtained with the different sensor configurations.

FIGURE 8: Assessment of sensor placements for several mCRE-based model updating problems.

that the presence of noise extends the identification issues on the less sensitive parameters of the problem, namely the top-story ones (W11, W21 and F20). Besides, if one compares the visual positioning of sensors previously shown with the relative confidence intervals widths, it appears that the subdomains of parameters having large intervals are not directly equipped by sensors (associated to poor local convexity of the functional and low sensitivity). One can also observe that the sensor placement configurations constrained to triaxial accelerometers are less efficient, as expected from the values of the determinant of the FIM plotted in the FSSP results.

The overall analysis of FIG. 8 confirms the effectiveness of mCRE-based OSP. Indeed, mCRE1 and mCRE2 sensor configurations provide the best parameter estimates, with minimal confidence intervals when data is noisy. This application is thus a proof-of-concept showing the benefits of FSSP with the modified FIM that directly yields from the interpretation of mCRE from a Bayesian viewpoint. Nevertheless, it is important to keep in mind the main limitation of this new OSP approach: the strong dependency in the confidence into measurements coefficient α . As running a mCRE-based OSP algorithm did not last more than 5 minutes for the considered case, the experimental designer can afford to assess mCRE-based OSPs obtained for several values of α . Despite this alternative, in-depth studies must be conducted to clarify this point. In particular, one can legitimately wonder if the optimality criteria for calibrating α that has been recently proposed in [80] are convenient to obtain relevant sensor configurations.

Finally, let us point out that taking into account several damage scenarios allows for a more robust sensor placement with respect to the identification of new parameter configurations, as shown in the FIG. 8 - mCRE-MS1 case at scenario (iii), where the identification is almost perfect with minimal confidence intervals. The computational time spent to "learn" the best

trade-off from multiple datasets is thus worth of interest. As one could have expected, taking into account several scenarios makes mCRE-MS1 and mCRE-MS2 model updating results sub-optimal (yet efficient) for cases (i) and (ii) compared to mCRE1 and mCRE2. However, the performance achieved in case (iii) by mCRE-MS1 and mCRE-MS2 is remarkable and promising for monitoring the occurrence and evolution of structural defects on structures. This observation goes in the sense of recent contributions [66, 70] which emphasize the need to take both model and measurement uncertainties into consideration to build efficient and robust OSP.

6. Conclusion and prospects

The ambition of this paper consisted in the development of a novel sensor placement algorithm that is dedicated to mCRE-based model updating. Owing to the link between the mCRE (though deterministic) and the Bayesian inference framework, and inspired from the Information Entropy concept, a modified Fisher Information Matrix was introduced and its determinant was maximized to optimally position sensors in the mCRE sense. A proof-of-concept showing the relevance of this new mCRE-based OSP strategy has been proposed on a 3D academic example where we sought for optimal accelerometers locations on a two-story frame structure subjected to random ground motion. This case study permitted to perform deep analysis of this new OSP approach and to compare it with other classical techniques in different model updating scenarios. In particular, the effect of the confidence into measurements coefficient has been emphasized, as well as the fact to take into consideration multiple scenarios so as to anticipate a wider range of potential damage occurrences. OSP methods were compared in terms of mCRE-based model updating from different datasets, which allowed to illustrate the efficiency and relevance of the proposed mCRE-based OSP methodology. If this study focuses on accelerometers as they are common and weakly invasive for earthquake engineering applications, all types of sensors can be easily integrated in the proposed framework.

Consequently, the proposed mCRE-based OSP appears as an interesting additional asset for the construction of a mCRE-unified framework for SHM or structural dynamics applications (see FIG. 9 for an example on how OSP could be combined to the recent publications of the authors [47, 75]). However, there is no doubt that this tool still lacks of maturity to be properly exploited, and further research should address the strong influence of the confidence into measurements coefficient [80]. Besides, as OSP are not exclusively intended to perform optimal model updating, future work will focus on finding the best sensor placement trade-off that contributes to multiple objectives simultaneously, for example modal identification and mCRE-based model updating. Pareto front algorithms may be a first tool for this purpose. Finally, one of the current on-going investigations of the authors concerns the use of mCRE-based OSP for active sensing purposes in order to improve damage detection in cases where the state of the structure is tracked online via data assimilation techniques [75]. Iterative strategies could then be employed to refine the sensor configuration only where needed, *i.e.* where damage occurrences are detected.

Appendix A Analytical expressions of the mCRE derivatives

Before providing gradient and Hessian matrix analytical expressions, let us recall that we are dealing with quantities written in the frequency domain. Therefore, derivatives must be considered with caution: the real and imaginary parts have to be separated to write consistent mathematical expressions (in particular Gateaux's derivatives). In the following, \bullet_r and \bullet_i will denote the real and imaginary parts of \bullet , respectively. Besides, indices ω will be omitted for the sake of clarity as all forthcoming developments are one at a given angular frequency ω . In particular, one can rewrite the system (16) so as to exhibit explicitly real and imaginary parts

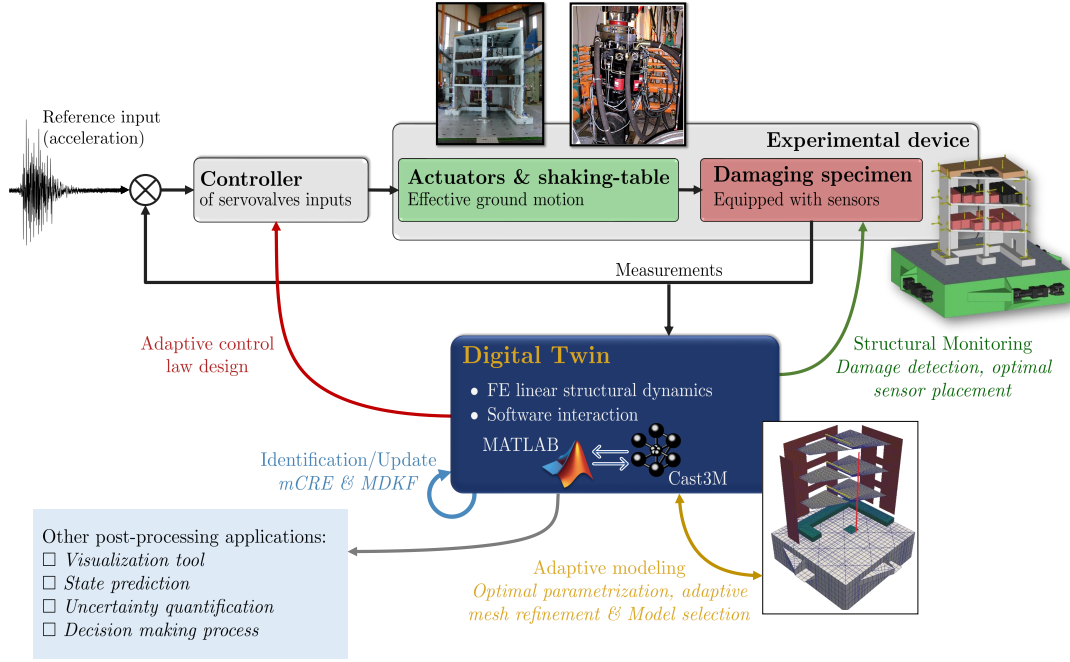


FIGURE 9: Long-term perspective: enhanced shaking-table experiments with a unified framework based on the modified Constitutive Relation Error.

of U and V in a decoupled manner:

$$\begin{aligned}
 A_{\text{ext}}(\theta)X_{\text{ext}} &= b_{\text{ext}} \text{ with} \\
 A_{\text{ext}}(\theta) &= \begin{bmatrix} K(\theta) - \omega^2 M + \alpha \Pi^T G \Pi & -(K(\theta) - \omega^2 M) & \omega D & -\omega D \\ -\omega^2 M & K(\theta) & -\omega D & 0 \\ -\omega D & \omega D & K(\theta) - \omega^2 M + \alpha \Pi^T G \Pi & -(K(\theta) - \omega^2 M) \\ \omega D & 0 & -\omega^2 M & K(\theta) \end{bmatrix} \quad (30) \\
 X_{\text{ext}}^T &= [U_r^T \quad V_r^T \quad U_i^T \quad V_i^T] \\
 b_{\text{ext}}^T &= [\alpha Y_r^T G \Pi \quad F_r^T \quad \alpha Y_i^T G \Pi \quad F_i^T]
 \end{aligned}$$

A.1 Analytical mCRE gradient

615 Once the mechanicals fields $\hat{s} = (U, V)$ are computed, the expression of the mCRE gradient with respect to the parameters to update can be analytical (only if the link between stiffness and parameters is too).

$$\begin{aligned}
 \left. \frac{de_{\omega}^2}{d\theta} \right|_{\hat{s}} &\triangleq \left. \frac{d\mathcal{L}}{d\theta} \right|_{\hat{s}} = \frac{\partial e_{\omega}^2}{\partial \theta} + \underbrace{\frac{\partial \mathcal{L}}{\partial U_r} \frac{dU_r}{d\theta} + \frac{\partial \mathcal{L}}{\partial V_r} \frac{dV_r}{d\theta} + \frac{\partial \mathcal{L}}{\partial U_i} \frac{dU_i}{d\theta} + \frac{\partial \mathcal{L}}{\partial V_i} \frac{dV_i}{d\theta}}_{= 0 \text{ at the saddle point}} \quad (31)
 \end{aligned}$$

As the parameters weight the FE stiffness matrix, a general formulation for the mCRE gradient with respect to parameter $\theta_k, k \in \llbracket 1; n_{\theta} \rrbracket$ is:

$$\left. \frac{de_{\omega}^2}{d\theta_k} \right|_{\hat{s}} = \frac{1}{2} \left[U_r^T \frac{\partial K}{\partial \theta_k} U_r + U_i^T \frac{\partial K}{\partial \theta_k} U_i - V_r^T \frac{\partial K}{\partial \theta_k} V_r - V_i^T \frac{\partial K}{\partial \theta_k} V_i \right] \quad (32)$$

For the stiffness parametrization (11), one thus directly gets:

$$\left. \frac{de_{\omega}^2}{d\theta_k} \right|_{\hat{s}} = \frac{1}{2} \left[U_r^T K_{0,k} U_r + U_i^T K_{0,k} U_i - V_r^T K_{0,k} V_r - V_i^T K_{0,k} V_i \right] \quad (33)$$

The possibility to provide an analytical gradient when minimizing the mCRE is thus strongly recommended due to its simplicity of implementation as well as the associated computational speed-up.

A.2 Semi-analytical Hessian matrix

Following the same idea, the mCRE Hessian matrix value at coordinate $j, k \in \llbracket 1; n_\theta \rrbracket^2$ reads:

$$\mathcal{H}_{jk}^\theta = \left. \frac{d^2 e_\omega^2}{d\theta_j d\theta_k} \right|_{\hat{s}} \triangleq \frac{d^2 \mathcal{L}}{d\theta_j d\theta_k} = \frac{\partial^2 \mathcal{L}}{\partial \theta_j \partial \theta_k} + \left[\frac{d}{dU_r} \left(\frac{\partial \mathcal{L}}{\partial \theta_k} \right) \right]^T \frac{dU_r}{d\theta_j} + \left[\frac{d}{dV_r} \left(\frac{\partial \mathcal{L}}{\partial \theta_k} \right) \right]^T \frac{dV_r}{d\theta_j} + \left[\frac{d}{dU_i} \left(\frac{\partial \mathcal{L}}{\partial \theta_k} \right) \right]^T \frac{dU_i}{d\theta_j} + \left[\frac{d}{dV_i} \left(\frac{\partial \mathcal{L}}{\partial \theta_k} \right) \right]^T \frac{dV_i}{d\theta_j} \quad (34)$$

620

Three terms to develop thus occur:

- The second order partial derivative of the augmented cost-function \mathcal{L} , which is trivial:

$$\frac{\partial^2 \mathcal{L}}{\partial \theta_j \partial \theta_k} = \frac{1}{2} \left[U_r^T \frac{\partial^2 K}{\partial \theta_j \partial \theta_k} U_r + U_i^T \frac{\partial^2 K}{\partial \theta_j \partial \theta_k} U_i - V_r^T \frac{\partial^2 K}{\partial \theta_j \partial \theta_k} V_r - V_i^T \frac{\partial^2 K}{\partial \theta_j \partial \theta_k} V_i \right] \quad (35)$$

- The crossed derivatives, whose computation is also direct:

$$\begin{cases} \frac{d}{dU_r} \left(\frac{\partial \mathcal{L}}{\partial \theta_k} \right) = \frac{\partial K}{\partial \theta_k} U_r \\ \frac{d}{dV_r} \left(\frac{\partial \mathcal{L}}{\partial \theta_k} \right) = -\frac{\partial K}{\partial \theta_k} V_r \\ \frac{d}{dU_i} \left(\frac{\partial \mathcal{L}}{\partial \theta_k} \right) = \frac{\partial K}{\partial \theta_k} U_i \\ \frac{d}{dV_i} \left(\frac{\partial \mathcal{L}}{\partial \theta_k} \right) = -\frac{\partial K}{\partial \theta_k} V_i \end{cases} \quad (36)$$

- The derivatives of \hat{s} with respect to parameters, whose computation can be obtained by derivation of the system $A_{\text{ext}} X_{\text{ext}} = b_{\text{ext}}$:

$$\frac{dA_{\text{ext}}}{d\theta_j} X_{\text{ext}} + A_{\text{ext}} \frac{dX_{\text{ext}}}{d\theta_j} = \frac{db_{\text{ext}}}{d\theta_j} \Rightarrow \frac{dX_{\text{ext}}}{d\theta_j} = A_{\text{ext}}^{-1} \left[\frac{db_{\text{ext}}}{d\theta_j} - \frac{dA_{\text{ext}}}{d\theta_j} X_{\text{ext}} \right] \quad (37)$$

with A_{ext}^{-1} that can be already known from the $A_{\text{ext}} X_{\text{ext}} = b_{\text{ext}}$ solution to compute the mCRE value (*i.e.* the inverse matrix can be stored) and:

$$\begin{cases} \frac{db_{\text{ext}}}{d\theta_j} = 0 \\ \frac{dA_{\text{ext}}}{d\theta_j} = \begin{bmatrix} \frac{\partial K}{\partial \theta_j} & -\frac{\partial K}{\partial \theta_j} & 0 & 0 \\ 0 & \frac{\partial K}{\partial \theta_j} & 0 & 0 \\ 0 & 0 & \frac{\partial K}{\partial \theta_j} & -\frac{\partial K}{\partial \theta_j} \\ 0 & 0 & 0 & \frac{\partial K}{\partial \theta_j} \end{bmatrix} \end{cases} \quad (38)$$

All simplifications done, one obtains:

$$\frac{d}{d\theta_j} \begin{bmatrix} U_r \\ V_r \\ U_i \\ V_i \end{bmatrix} = -A_{\text{ext}}^{-1} \begin{bmatrix} \frac{\partial K}{\partial \theta_j} (U_r - V_r) \\ \frac{\partial K}{\partial \theta_j} V_r \\ \frac{\partial K}{\partial \theta_j} (U_i - V_i) \\ \frac{\partial K}{\partial \theta_j} V_i \end{bmatrix} \quad (39)$$

Finally, the general expression of \mathcal{H}_{jk}^θ reads:

$$\mathcal{H}_{jk}^\theta = \frac{1}{2} \left[U_r^T \frac{\partial^2 K}{\partial \theta_j \partial \theta_k} U_r + U_i^T \frac{\partial^2 K}{\partial \theta_j \partial \theta_k} U_i - V_r^T \frac{\partial^2 K}{\partial \theta_j \partial \theta_k} V_r - V_i^T \frac{\partial^2 K}{\partial \theta_j \partial \theta_k} V_i \right] - \begin{bmatrix} \frac{\partial K}{\partial \theta_k} U_r \\ -\frac{\partial K}{\partial \theta_k} V_r \\ \frac{\partial K}{\partial \theta_k} U_i \\ -\frac{\partial K}{\partial \theta_k} V_i \end{bmatrix}^T A_{\text{ext}}^{-1} \begin{bmatrix} \frac{\partial K}{\partial \theta_j} (U_r - V_r) \\ \frac{\partial K}{\partial \theta_j} V_r \\ \frac{\partial K}{\partial \theta_j} (U_i - V_i) \\ \frac{\partial K}{\partial \theta_j} V_i \end{bmatrix} \quad (40)$$

The application of this expression to the stiffness parametrization (11) leads to:

$$\mathcal{H}_{jk}^\theta = - \begin{bmatrix} K_{0,k} U_r \\ -K_{0,k} V_r \\ K_{0,k} U_i \\ -K_{0,k} V_i \end{bmatrix}^T A_{\text{ext}}^{-1} \begin{bmatrix} K_{0,j} (U_r - V_r) \\ K_{0,j} V_r \\ K_{0,j} (U_i - V_i) \\ K_{0,j} V_i \end{bmatrix} \quad (41)$$

If the expression of the mCRE gradient is easily available (according to the stiffness parametrization), the mCRE gradient with respect to updated parameters must be provided to minimization algorithms in order to get enhanced numerical performances. The case of the Hessian matrix is a bit different due to the fact that it requires intelligent storage of the inverse matrix of A_{ext} for all $\omega \in D_\omega$. In particular, one can notice that A is inverted instead of A_{ext} due to its reduced size. Of course, providing the Hessian would also reduce the amount of iterations of nonlinear optimization algorithms but it also carries a storage burden that should be taken into account as A_{ext}^{-1} must be stored and differs for all $\omega \in D_\omega$.

Appendix B Confidence intervals to assess mCRE-based model updating in terms of relative uncertainty

As explained in [53], providing optimal parameters inside confidence intervals is an original and effective way to deal with the uncertainty associated with the FE model as well as excitation levels with a low computational cost, as it is a one-step direct post-processing procedure to perform once the model updating algorithm has minimized the mCRE functional \mathcal{J} . At the converged point $\hat{\theta}$, using the convexity properties of the functional, there exists a subset $I_\theta \subset \Theta$ of finite size such that:

$$\forall \theta \in I_\theta, \quad \mathcal{J}(\theta) < \epsilon \mathcal{J}(\hat{\theta}) \quad (42)$$

where ϵ is a constant scalar. The width of I_θ for a given threshold ϵ can be established using a second order Taylor polynomial approximation around the optimal parameters $\hat{\theta}$:

$$\mathcal{J}(\theta) = J(\theta) + \mathcal{O}\left((\theta - \hat{\theta})^3\right) \quad \text{with} \quad J(\theta) = \mathcal{J}(\hat{\theta}) + \left[\frac{d\mathcal{J}}{d\theta} \right]^T (\theta - \hat{\theta}) + \frac{1}{2} (\theta - \hat{\theta})^T \left[\frac{d^2\mathcal{J}}{d\theta^2} \right] (\theta - \hat{\theta}) \quad (43)$$

Once gradient and Hessian matrix are supplied, the 2nd order approximation of the mCRE is directly available, which allows to calculate the size of I_θ for all parameters (ϵ has to be user-defined).

Note that the proposed confidence intervals are not rigorously able to quantify uncertainties on $\hat{\theta}$. Nonetheless, they are enough to draw preliminary conclusions about the relative ability to identify parameters: comparing the relative width of confidence intervals allows to assess which parameters are subjected to more doubt than others. This can be helpful if one wants to focus model updating actions on exclusively highly-sensitive parameters in order to avoid physically-meaningless local minima.

640 **References**

- [1] J. Brownjohn, [Structural health monitoring of civil infrastructure](#), Philosophical Transactions of the Royal Society A: Mathematical, Physical and Engineering Sciences 365 (1851) (2007) 589–622. doi:10.1098/rsta.2006.1925.
URL <https://royalsocietypublishing.org/doi/10.1098/rsta.2006.1925>
- 645 [2] S. Laflamme, L. Cao, E. Chatzi, F. Ubertini, [Damage Detection and Localization from Dense Network of Strain Sensors](#), Shock and Vibration 2016 (2016) 1–13. doi:10.1155/2016/2562949.
URL <http://www.hindawi.com/journals/sv/2016/2562949/>
- [3] G. F. Gomes, Y. A. D. Mendez, P. da Silva Lopes Alexandrino, S. S. da Cunha, A. C. Ancelotti, [A Review of Vibration Based Inverse Methods for Damage Detection and Identification in Mechanical Structures Using Optimization Algorithms and ANN](#), Archives of Computational Methods in Engineering 26 (4) (2019) 883–897. doi:10.1007/s11831-018-9273-4.
650 URL <https://doi.org/10.1007/s11831-018-9273-4>
- [4] E. N. Chatzi, M. N. Chatzis, C. Papadimitriou (Eds.), Robust Monitoring, Diagnostic Methods and Tools for Engineered Systems, Frontiers Research Topics, Frontiers Media SA, 2020. doi:10.3389/978-2-88966-088-9.
655 URL <https://doi.org/10.3389/978-2-88966-088-9>
- [5] E. Simoen, G. De Roeck, G. Lombaert, [Dealing with uncertainty in model updating for damage assessment: A review](#), Mechanical Systems and Signal Processing 56-57 (2015) 123–149. doi:10.1016/j.ymsp.2014.11.001.
URL <https://linkinghub.elsevier.com/retrieve/pii/S0888327014004130>
- 660 [6] W. Fan, P. Qiao, [Vibration-based Damage Identification Methods: A Review and Comparative Study](#), Structural Health Monitoring 10 (1) (2011) 83–111, publisher: SAGE Publications. doi:10.1177/1475921710365419.
URL <https://doi.org/10.1177/1475921710365419>
- [7] J. E. Mottershead, M. I. Friswell, [Model Updating In Structural Dynamics: A Survey](#), Journal of Sound and Vibration 167 (2) (1993) 347–375. doi:10.1006/jsvi.1993.1340.
665 URL <https://www.sciencedirect.com/science/article/pii/S0022460X83713404>
- [8] A. Tarantola, [Inverse Problem Theory and Methods for Model Parameter Estimation](#), Society for Industrial and Applied Mathematics, 2005. doi:10.1137/1.9780898717921.
URL <http://epubs.siam.org/doi/book/10.1137/1.9780898717921>
- 670 [9] M. I. Friswell, [Damage identification using inverse methods](#), Philosophical Transactions of the Royal Society A: Mathematical, Physical and Engineering Sciences 365 (1851) (2007) 393–410. doi:10.1098/rsta.2006.1930.
URL <https://royalsocietypublishing.org/doi/10.1098/rsta.2006.1930>
- [10] A. Bensoussan, [Optimization of sensor’s location in a distributed filtering problem., Stability of stochastic dynamical systems \(1972\)](#) 62–84.
675
- [11] T. K. Yu, J. H. Seinfeld, [Observability and optimal measurement location in linear distributed parameter systems](#), International Journal of Control 18 (4) (1973) 785–799, publisher: Taylor & Francis _eprint: <https://doi.org/10.1080/00207177308932556>. doi:10.1080/00207177308932556.
URL <https://doi.org/10.1080/00207177308932556>
- 680 [12] T.-H. Yi, H.-N. Li, [Methodology Developments in Sensor Placement for Health Monitoring of Civil Infrastructures](#), International Journal of Distributed Sensor Networks 8 (8) (2012) 612726, publisher: SAGE Publications. doi:10.1155/2012/612726.
URL <https://doi.org/10.1155/2012/612726>
- [13] V. Mallardo, M. Aliabadi, [Optimal Sensor Placement for Structural, Damage and Impact Identification: A Review](#), Structural Durability & Health Monitoring 9 (4) (2013) 287–323. doi:10.32604/sdhm.2013.009.287.
685 URL <http://www.techscience.com/sdhm/v9n4/35096>
- [14] W. Ostachowicz, R. Soman, P. Malinowski, [Optimization of sensor placement for structural health monitoring: a review](#), Structural Health Monitoring 18 (3) (2019) 963–988, publisher: SAGE Publications. doi:10.1177/1475921719825601.
690 URL <https://doi.org/10.1177/1475921719825601>

- [15] R. J. Barthorpe, K. Worden, [Emerging Trends in Optimal Structural Health Monitoring System Design: From Sensor Placement to System Evaluation](#), Journal of Sensor and Actuator Networks 9 (3) (2020) 31, number: 3 Publisher: Multidisciplinary Digital Publishing Institute. doi:10.3390/jsan9030031.
695 URL <https://www.mdpi.com/2224-2708/9/3/31>
- [16] P. C. Shah, F. E. Udawadia, [A Methodology for Optimal Sensor Locations for Identification of Dynamic Systems](#), Journal of Applied Mechanics 45 (1) (1978) 188–196. doi:10.1115/1.3424225.
URL <https://doi.org/10.1115/1.3424225>
- [17] P. Cawley, R. D. Adams, [The location of defects in structures from measurements of natural frequencies](#), The Journal of Strain Analysis for Engineering Design 14 (2) (1979) 49–57, publisher: IMECHE. doi:10.1243/03093247V142049.
700 URL <https://doi.org/10.1243/03093247V142049>
- [18] P. Kirkegaard, R. Brincker, [On the optimal location of sensors for parametric identification of linear structural systems](#), Mechanical Systems and Signal Processing 8 (6) (1994) 639–647. doi:10.1006/mssp.1994.1045.
705 URL <https://linkinghub.elsevier.com/retrieve/pii/S0888327084710454>
- [19] D. C. Kammer, [Sensor placement for on-orbit modal identification and correlation of large space structures](#), Journal of Guidance, Control, and Dynamics 14 (2) (1991) 251–259. doi:10.2514/3.20635.
URL <https://arc.aiaa.org/doi/abs/10.2514/3.20635>
- [20] E. Heredia-Zavoni, L. Esteva, [Optimal instrumentation of uncertain structural systems subject to earthquake ground motions](#), Earthquake Engineering & Structural Dynamics 27 (4) (1998) 343–362. doi:10.1002/(SICI)1096-9845(199804)27:4<343::AID-EQE726>3.0.CO;2-F.
710 URL <https://onlinelibrary.wiley.com/doi/abs/10.1002/%28SICI%291096-9845%28199804%2927%3A4%3C343%3A%3AAID-EQE726%3E3.0.CO%3B2-F>
- [21] F. E. Udawadia, [Methodology for Optimum Sensor Locations for Parameter Identification in Dynamic Systems](#), Journal of Engineering Mechanics 120 (2) (1994) 368–390, publisher: American Society of Civil Engineers. doi:10.1061/(ASCE)0733-9399(1994)120:2(368).
715 URL <https://ascelibrary.org/doi/abs/10.1061/%28ASCE%290733-9399%281994%29120%3A2%28368%29>
- [22] E. Heredia-Zavoni, R. Montes-Iturrizaga, L. Esteva, [Optimal instrumentation of structures on flexible base for system identification](#), Earthquake Engineering & Structural Dynamics 28 (12) (1999) 1471–1482. doi:10.1002/(SICI)1096-9845(199912)28:12<1471::AID-EQE872>3.0.CO;2-M.
720 URL <https://onlinelibrary.wiley.com/doi/abs/10.1002/%28SICI%291096-9845%28199912%2928%3A12%3C1471%3A%3AAID-EQE872%3E3.0.CO%3B2-M>
- [23] M. Reynier, H. Abou-kandil, [Sensors Location For Updating Problems](#), Mechanical Systems and Signal Processing 13 (2) (1999) 297–314. doi:10.1006/mssp.1998.1213.
725 URL <https://www.sciencedirect.com/science/article/pii/S0888327098912134>
- [24] L. Yao, W. A. Sethares, D. C. Kammer, [Sensor placement for on-orbit modal identification via a genetic algorithm](#), AIAA Journal 31 (10) (1993) 1922–1928, publisher: American Institute of Aeronautics and Astronautics eprint: <https://doi.org/10.2514/3.11868>. doi:10.2514/3.11868.
URL <https://doi.org/10.2514/3.11868>
- [25] J. L. Beck, L. S. Katafygiotis, [Updating Models and Their Uncertainties. I: Bayesian Statistical Framework](#), Journal of Engineering Mechanics 124 (4) (1998) 455–461, publisher: American Society of Civil Engineers. doi:10.1061/(ASCE)0733-9399(1998)124:4(455).
730 URL <https://ascelibrary.org/doi/abs/10.1061/%28ASCE%290733-9399%281998%29124%3A4%28455%29>
- [26] L. S. Katafygiotis, J. L. Beck, [Updating Models and Their Uncertainties. II: Model Identifiability](#), Journal of Engineering Mechanics 124 (4) (1998) 463–467, publisher: American Society of Civil Engineers. doi:10.1061/(ASCE)0733-9399(1998)124:4(463).
735 URL <https://ascelibrary.org/doi/abs/10.1061/%28ASCE%290733-9399%281998%29124%3A4%28463%29>
- [27] C. Papadimitriou, J. L. Beck, S.-K. Au, [Entropy-Based Optimal Sensor Location for Structural Model Updating](#), Journal of Vibration and Control 6 (5) (2000) 781–800, publisher: SAGE Publications Ltd STM. doi:10.1177/107754630000600508.
740 URL <https://doi.org/10.1177/107754630000600508>
- [28] C. Papadimitriou, [Optimal sensor placement methodology for parametric identification of structural systems](#), Journal of Sound and Vibration 278 (4) (2004) 923–947. doi:10.1016/j.jsv.2003.10.063.
URL <https://www.sciencedirect.com/science/article/pii/S0022460X04000355>

- 745 [29] H. Y. Guo, L. Zhang, L. L. Zhang, J. X. Zhou, [Optimal placement of sensors for structural health monitoring using improved genetic algorithms](#), *Smart Materials and Structures* 13 (3) (2004) 528–534, publisher: IOP Publishing. doi:10.1088/0964-1726/13/3/011.
URL <https://doi.org/10.1088/0964-1726/13/3/011>
- [30] A. Mendler, M. Dähler, C. E. Ventura, [Sensor placement with optimal damage detectability for statistical damage detection](#), *Mechanical Systems and Signal Processing* 170 (2022) 108767. doi:10.1016/j.ymsp.2021.108767.
URL <https://www.sciencedirect.com/science/article/pii/S0888327021010815>
- [31] K. Worden, A. P. Burrows, [Optimal sensor placement for fault detection](#), *Engineering Structures* 23 (8) (2001) 885–901. doi:10.1016/S0141-0296(00)00118-8.
755 URL <https://www.sciencedirect.com/science/article/pii/S0141029600001188>
- [32] M. Azarbajegani, A. I. El-Osery, K. K. Choi, M. M. R. Taha, [A probabilistic approach for optimal sensor allocation in structural health monitoring](#), *Smart Materials and Structures* 17 (5) (2008) 055019, publisher: IOP Publishing. doi:10.1088/0964-1726/17/5/055019.
URL <https://doi.org/10.1088/0964-1726/17/5/055019>
- 760 [33] M. Bruggi, S. Mariani, [Optimization of sensor placement to detect damage in flexible plates](#), *Engineering Optimization* 45 (6) (2013) 659–676, publisher: Taylor & Francis eprint: <https://doi.org/10.1080/0305215X.2012.690870>. doi:10.1080/0305215X.2012.690870.
URL <https://doi.org/10.1080/0305215X.2012.690870>
- [34] B. Blachowski, M. Ostrowski, P. Tazowski, A. Swiercz, L. Jankowski, [Sensor placement for structural damage identification by means of topology optimization](#), *AIP Conference Proceedings* 2239 (1) (2020) 020002, publisher: American Institute of Physics. doi:10.1063/5.0007817.
765 URL <https://aip.scitation.org/doi/abs/10.1063/5.0007817>
- [35] D. Nasr, R. E. Dahr, J. Assaad, J. Khatib, [Comparative Analysis between Genetic Algorithm and Simulated Annealing-Based Frameworks for Optimal Sensor Placement and Structural Health Monitoring Purposes](#), *Buildings* 12 (9) (2022) 1383. doi:10.3390/buildings12091383.
770 URL <https://www.mdpi.com/2075-5309/12/9/1383>
- [36] J. M. Beal, A. Shukla, O. A. Brezhneva, M. A. Abramson, [Optimal sensor placement for enhancing sensitivity to a change in stiffness for structural health monitoring](#), *Optimization and Engineering* 9 (2) (2008) 119–142. doi:10.1007/s11081-007-9023-1.
775 URL <https://doi.org/10.1007/s11081-007-9023-1>
- [37] C. Papadimitriou, [Pareto optimal sensor locations for structural identification](#), *Computer Methods in Applied Mechanics and Engineering* 194 (12) (2005) 1655–1673. doi:10.1016/j.cma.2004.06.043.
URL <https://www.sciencedirect.com/science/article/pii/S0045782504004104>
- [38] C. Papadimitriou, G. Lombaert, [The effect of prediction error correlation on optimal sensor placement in structural dynamics](#), *Mechanical Systems and Signal Processing* 28 (2012) 105–127. doi:10.1016/j.ymsp.2011.05.019.
780 URL <https://linkinghub.elsevier.com/retrieve/pii/S0888327011002214>
- [39] J. Waeytens, B. Rosić, P.-E. Charbonnel, E. Merliot, D. Siegert, X. Chapeleau, R. Vidal, V. le Corvec, L.-M. Cottineau, [Model updating techniques for damage detection in concrete beam using optical fiber strain measurement device](#), *Engineering Structures* 129 (2016) 2–10. doi:10.1016/j.engstruct.2016.08.004.
785 URL <https://linkinghub.elsevier.com/retrieve/pii/S0141029616304059>
- [40] M. Ben Azzouna, P. Feissel, P. Villon, [Robust identification of elastic properties using the Modified Constitutive Relation Error](#), *Computer Methods in Applied Mechanics and Engineering* 295 (2015) 196–218. doi:10.1016/j.cma.2015.04.004.
790 URL <https://linkinghub.elsevier.com/retrieve/pii/S0045782515001486>
- [41] J. E. Mottershead, M. Link, M. I. Friswell, [The sensitivity method in finite element model updating: A tutorial](#), *Mechanical Systems and Signal Processing* 25 (7) (2011) 2275–2296. doi:10.1016/j.ymsp.2010.10.012.
URL <https://linkinghub.elsevier.com/retrieve/pii/S0888327010003316>
- 795 [42] B. Weber, P. Paultre, J. Proulx, [Consistent regularization of nonlinear model updating for damage identification](#), *Mechanical Systems and Signal Processing* 23 (6) (2009) 1965–1985. doi:10.1016/j.ymsp.2008.04.011.
URL <https://www.sciencedirect.com/science/article/pii/S088832700800109X>

- [43] C. D. Zhang, Y. L. Xu, [Comparative studies on damage identification with Tikhonov regularization and sparse regularization: Damage Detection with Tikhonov Regularization and Sparse Regularization](#), *Structural Control and Health Monitoring* 23 (3) (2016) 560–579. doi:10.1002/stc.1785.
URL <https://onlinelibrary.wiley.com/doi/10.1002/stc.1785>
- [44] B. Titurus, M. I. Friswell, [Regularization in model updating](#), *International Journal for Numerical Methods in Engineering* 75 (4) (2008) 440–478. doi:10.1002/nme.2257.
URL <https://onlinelibrary.wiley.com/doi/10.1002/nme.2257>
- [45] S. Huang, P. Feissel, P. Villon, [Modified constitutive relation error: An identification framework dealing with the reliability of information](#), *Computer Methods in Applied Mechanics and Engineering* 311 (2016) 1–17. doi:10.1016/j.cma.2016.06.030.
URL <https://linkinghub.elsevier.com/retrieve/pii/S0045782516306557>
- [46] T. Silva, N. Maia, [Detection and localisation of structural damage based on the error in the constitutive relations in dynamics](#), *Applied Mathematical Modelling* 46 (2017) 736–749. doi:10.1016/j.apm.2016.07.002.
URL <https://linkinghub.elsevier.com/retrieve/pii/S0307904X16303833>
- [47] M. Diaz, P.-E. Charbonnel, L. Chamoin, [Robust energy-based model updating framework for random processes in dynamics: application to shaking-table experiments](#), *Computers and Structures* 264 (106746) (2022) 40. doi:https://doi.org/10.1016/j.compstruc.2022.106746.
- [48] A. T. Chouaki, P. Ladevèze, L. Proslir, [Updating Structural Dynamic Models with Emphasis on the Damping Properties](#), *AIAA Journal* 36 (6) (1998) 1094–1099, publisher: American Institute of Aeronautics and Astronautics eprint: <https://doi.org/10.2514/2.486>. doi:10.2514/2.486.
URL <https://doi.org/10.2514/2.486>
- [49] P. Ladevèze, A. Chouaki, [Application of a posteriori error estimation for structural model updating](#), *Inverse Problems* 15 (1) (1999) 49–58, publisher: IOP Publishing. doi:10.1088/0266-5611/15/1/009.
URL <https://doi.org/10.1088/0266-5611/15/1/009>
- [50] P. Ladevèze, D. Leguillon, [Error Estimate Procedure in the Finite Element Method and Applications](#), *SIAM Journal on Numerical Analysis* 20 (3) (1983) 485–509, publisher: Society for Industrial and Applied Mathematics. doi:10.1137/0720033.
URL <https://epubs.siam.org/doi/10.1137/0720033>
- [51] W. Aquino, M. Bonnet, [Analysis of the error in constitutive equation approach for time-harmonic elasticity imaging](#), *SIAM Journal on Applied Mathematics* 79 (3) (2019) 822–849. arXiv:<https://doi.org/10.1137/18M1231237>, doi:10.1137/18M1231237.
URL <https://doi.org/10.1137/18M1231237>
- [52] P. Feissel, O. Allix, [Modified constitutive relation error identification strategy for transient dynamics with corrupted data: The elastic case](#), *Computer Methods in Applied Mechanics and Engineering* 196 (13-16) (2007) 1968–1983. doi:10.1016/j.cma.2006.10.005.
URL <https://linkinghub.elsevier.com/retrieve/pii/S0045782506003434>
- [53] P. Charbonnel, P. Ladevèze, F. Louf, C. Le Noac’h, [A robust CRE-based approach for model updating using in situ measurements](#), *Computers & Structures* 129 (2013) 63–73. doi:10.1016/j.compstruc.2013.08.002.
URL <https://linkinghub.elsevier.com/retrieve/pii/S0045794913002216>
- [54] E. Barbarella, O. Allix, F. Daghia, J. Lamon, T. Jollivet, [A new inverse approach for the localization and characterization of defects based on compressive experiments](#), *Computational Mechanics* 57 (6) (2016) 1061–1074. doi:10.1007/s00466-016-1278-y.
URL <http://link.springer.com/10.1007/s00466-016-1278-y>
- [55] X. Hu, S. Prabhu, S. Atamturktur, S. Cogan, [Mechanistically-informed damage detection using dynamic measurements: Extended constitutive relation error](#), *Mechanical Systems and Signal Processing* 85 (2017) 312–328. doi:10.1016/j.ymssp.2016.08.013.
URL <https://linkinghub.elsevier.com/retrieve/pii/S0888327016302965>
- [56] B. Banerjee, T. F. Walsh, W. Aquino, M. Bonnet, [Large scale parameter estimation problems in frequency-domain elastodynamics using an error in constitutive equation functional](#), *Computer Methods in Applied Mechanics and Engineering* 253 (2013) 60–72. doi:10.1016/j.cma.2012.08.023.
URL <https://linkinghub.elsevier.com/retrieve/pii/S0045782512002770>

- [57] R. Ferrier, A. Cocchi, C. Hochard, [Modified constitutive relation error for field identification: Theoretical and experimental assessments on fiber orientation identification in a composite material](#), *International Journal for Numerical Methods in Engineering* (2021). doi:10.1002/nme.6842.
URL <https://onlinelibrary.wiley.com/doi/10.1002/nme.6842>
- 855 [58] D. C. Kammer, [Effect of model error on sensor placement for on-orbit modal identification of large space structures](#), *Journal of Guidance, Control, and Dynamics* 15 (2) (1992) 334–341, publisher: American Institute of Aeronautics and Astronautics .eprint: <https://doi.org/10.2514/3.20841>. doi:10.2514/3.20841.
URL <https://doi.org/10.2514/3.20841>
- [59] D. C. Kammer, [Effects of Noise on Sensor Placement for On-Orbit Modal Identification of Large Space Structures](#), *Journal of Dynamic Systems, Measurement, and Control* 114 (3) (1992) 436–443. doi:10.1115/1.2897366.
860 URL <https://doi.org/10.1115/1.2897366>
- [60] D. C. Kammer, M. L. Tinker, [Optimal placement of triaxial accelerometers for modal vibration tests](#), *Mechanical Systems and Signal Processing* 18 (1) (2004) 29–41. doi:10.1016/S0888-3270(03)00017-7.
865 URL <https://www.sciencedirect.com/science/article/pii/S0888327003000177>
- [61] Z. Y. Shi, S. S. Law, L. M. Zhang, [Optimum Sensor Placement for Structural Damage Detection](#), *Journal of Engineering Mechanics* 126 (11) (2000) 1173–1179, publisher: American Society of Civil Engineers. doi:10.1061/(ASCE)0733-9399(2000)126:11(1173).
URL <https://ascelibrary.org/doi/abs/10.1061/%28ASCE%290733-9399%282000%29126%3A11%281173%29>
- 870 [62] B. Blachowski, [Modal Sensitivity Based Sensor Placement for Damage Identification Under Sparsity Constraint](#), *Periodica Polytechnica Civil Engineering* (Mar. 2019). doi:10.3311/PPci.13888.
URL <https://pp.bme.hu/ci/article/view/13888>
- [63] M. Salama, T. Rose, J. Garba, [Optimal placement of excitations and sensors for verification of large dynamical systems](#), in: 28th Structures, Structural Dynamics and Materials Conference, American Institute of Aeronautics and Astronautics, 1987. doi:<https://doi.org/10.2514/6.1987-782>.
875 URL <https://arc.aiaa.org/doi/abs/10.2514/6.1987-782>
- [64] D. S. Li, H. N. Li, C. P. Fritzen, [The connection between effective independence and modal kinetic energy methods for sensor placement](#), *Journal of Sound and Vibration* 305 (4) (2007) 945–955. doi:10.1016/j.jsv.2007.05.004.
880 URL <https://www.sciencedirect.com/science/article/pii/S0022460X07003537>
- [65] K.-V. Yuen, L. S. Katafygiotis, C. Papadimitriou, N. C. Mickleborough, [Optimal Sensor Placement Methodology for Identification with Unmeasured Excitation](#), *Journal of Dynamic Systems, Measurement, and Control* 123 (4) (2001) 677–686. doi:10.1115/1.1410929.
URL <https://doi.org/10.1115/1.1410929>
- 885 [66] S. Cantero-Chinchilla, J. L. Beck, M. Chiachío, J. Chiachío, D. Chronopoulos, A. Jones, [Optimal sensor and actuator placement for structural health monitoring via an efficient convex cost-benefit optimization](#), *Mechanical Systems and Signal Processing* 144, publisher: Elsevier (Apr. 2020). doi:10.1016/j.ymsp.2020.106901.
- [67] P. Metallidis, G. Verros, S. Natsiavas, C. Papadimitriou, [Fault Detection and Optimal Sensor Location in Vehicle Suspensions](#), *Journal of Vibration and Control* 9 (3-4) (2003) 337–359, publisher: SAGE Publications Ltd STM. doi:10.1177/107754603030755.
890 URL <https://doi.org/10.1177/107754603030755>
- [68] Q. Long, M. Motamed, R. Tempone, [Fast Bayesian optimal experimental design for seismic source inversion](#), *Computer Methods in Applied Mechanics and Engineering* 291 (2015) 123–145. doi:10.1016/j.cma.2015.03.021.
895 URL <https://www.sciencedirect.com/science/article/pii/S0045782515001310>
- [69] C. Argyris, S. Chowdhury, V. Zabel, C. Papadimitriou, [Bayesian optimal sensor placement for crack identification in structures using strain measurements](#), *Structural Control and Health Monitoring* 25 (5) (2018) e2137. doi:10.1002/stc.2137.
900 URL <https://onlinelibrary.wiley.com/doi/abs/10.1002/stc.2137>
- [70] T. Ercan, C. Papadimitriou, [Optimal Sensor Placement for Reliable Virtual Sensing Using Modal Expansion and Information Theory](#), *Sensors* 21 (10) (2021) 3400, number: 10 Publisher: Multidisciplinary Digital Publishing Institute. doi:10.3390/s21103400.
URL <https://www.mdpi.com/1424-8220/21/10/3400>

- 905 [71] A. Deraemaeker, P. Ladevèze, P. Leconte, [Reduced bases for model updating in structural dynamics based on constitutive relation error](#), *Computer Methods in Applied Mechanics and Engineering* 191 (21-22) (2002) 2427–2444. doi:10.1016/S0045-7825(01)00421-2.
URL <https://linkinghub.elsevier.com/retrieve/pii/S0045782501004212>
- [72] B. Marchand, L. Chamoin, C. Rey, [Parameter identification and model updating in the context of nonlinear mechanical behaviors using a unified formulation of the modified Constitutive Relation Error concept](#), *Computer Methods in Applied Mechanics and Engineering* 345 (2019) 1094–1113. doi:10.1016/j.cma.2018.09.008.
910 URL <https://linkinghub.elsevier.com/retrieve/pii/S0045782518304511>
- [73] A. Deraemaeker, P. Ladevèze, T. Romeuf, [Model validation in the presence of uncertain experimental data](#), *Engineering Computations* 21 (8) (2004) 808–833. doi:10.1108/02644400410554335.
915 URL <https://www.emerald.com/insight/content/doi/10.1108/02644400410554335/full/html>
- [74] H. N. Nguyen, L. Chamoin, C. Ha Minh, [mcre-based parameter identification from full-field measurements: Consistent framework, integrated version, and extension to nonlinear material behaviors](#), *Computer Methods in Applied Mechanics and Engineering* 400 (2022) 115461. doi:https://doi.org/10.1016/j.cma.2022.115461.
920 URL <https://www.sciencedirect.com/science/article/pii/S0045782522004947>
- [75] M. Diaz, P.-E. Charbonnel, L. Chamoin, [A new kalman filter approach for structural parameter tracking: Application to the monitoring of damaging structures tested on shaking-tables](#), *Mechanical Systems and Signal Processing* 182 (2023) 109529. doi:https://doi.org/10.1016/j.ymsp.2022.109529.
925 URL <https://www.sciencedirect.com/science/article/pii/S088832702200632X>
- [76] P.-E. Charbonnel, [Fuzzy-driven strategy for fully automated modal analysis: Application to the SMART2013 shaking-table test campaign](#), *Mechanical Systems and Signal Processing* 152 (2021) 107388. doi:10.1016/j.ymsp.2020.107388.
URL <https://linkinghub.elsevier.com/retrieve/pii/S0888327020307743>
- 930 [77] Cast3M, <http://www-cast3m.cea.fr>.
- [78] C. Y. Shih, Y. G. Tsuei, R. J. Allemang, D. L. Brown, [Complex mode indication function and its applications to spatial domain parameter estimation](#), *Mechanical Systems and Signal Processing* 2 (4) (1988) 367–377. doi:10.1016/0888-3270(88)90060-X.
URL <https://www.sciencedirect.com/science/article/pii/088832708890060X>
- 935 [79] R. J. Allemang, D. L. Brown, [A Complete Review of the Complex Mode Indicator Function \(CMIF\) with Applications](#) (2006) 38.
URL [https://www.semanticscholar.org/paper/A-Complete-Review-of-the-Complex-Mode-Indicator-\(-\)-Allemang-Brown/5184ead6fcde301507bad9aa09b6bce08d97dceb](https://www.semanticscholar.org/paper/A-Complete-Review-of-the-Complex-Mode-Indicator-(-)-Allemang-Brown/5184ead6fcde301507bad9aa09b6bce08d97dceb)
- [80] M. Diaz, P.-É. Charbonnel, L. Chamoin, [Fully automated physics-regularized model updating algorithm for vibration-based damage detection from sparse data](#) Submitted - preprint available on HAL (03872031) (2022).
940